An Adaptable Robotic Snake using a Compliant Actuated Tensegrity Structure for Locomotion and its Motion Pattern Analysis

Qi He
Msc by Research
University of York
Electronic Engineering

January 4, 2021

Abstract

The thesis explores the possibilities that using a compliant actuated tensegrity structure to build an adapted robotic snake for locomotion. With the development of modern society, people are relying more and more on robots to assist in their work. The robotic snake is a type of robot that is often used in exploration and relief work on complex terrain due to its unique bionic structure. However, traditional snake-like robots have structures that focus on specific snake-like movement patterns, but cannot actually simulate how the spine and muscles of a snake can work, thus losing out on desirable features such as high energy efficiency and flexibility.

In this work, a tensegrity structure is researched to enable a robotic snake to realize the structure and capabilities of a snake. A prototype has been built for experiments: three segments connected by springs and strings which forms a tension network. The prototype is actuated by the change of the tension within the network, just as the muscles in a snake contract and stretch around the spine. Experiments with the prototype show that it can carry out effective rectilinear movement and steering movement on a variety of terrain, and its overall speed is mainly limited by the friction coefficient of the ground. However, because the underside of the body module prevents the module from tilting, the prototype cannot perform serpentine movement. More improvements in the shape design of the body modules and motion control could also be studied in future work.

Contents

List of Tables

List of Figures

Acknowledgements

Firstly, I would like to express my most sincere gratitude to my supervisor, Dr. Mark A. Post, for his valuable suggestions and help with my research, without which much of this work would not have been possible, especially during the COVID-19, many work has been hindered.

Further thanks to my second supervisor Dr. Andy Tyrrell for his guidance and help throughout this year of my research. I also want to say thanks to all the members of the Robot Lab, for their help and sharing throughout this year of research.

Finally, my deep gratitude goes to my family for their unconditional support, end-less love and encouragement.

Declaration

I declare that this thesis is a presentation of original work and I am the sole author. This work has not previously been presented for an award at this, or any other, University. All sources are acknowledged as References.

1 Introduction

This chapter describes the motivation behind the research, as well as the preliminary hypothesis. Subsequent chapters are also described simply in Section 1.2.

1.1 Thesis Overview

In spite of the advances that have occurred in robotic snake research, the majority of snake-like robots are based on sturctures that imitate the motion of a snake. However, it is worth noting that such a mechanism, though simple, does not provide rich degrees of freedom, leaving the bionics of the robot snake at a superficial level and resulting in the musculoskeletal structure of such a snake being difficult to simulate and ineffective.

The hypothesis of this project is that creating a structure similar to a snake's musculoskeletal structure would make the robot more adaptable to different environments by improving the bionic properties. If this is indeed the case, it will most likely be because the musculoskeletal tension structure better transfers the force in space. Under the premise of maintaining multiple degrees of freedom, the robotic snake can keep maintaining pretension, which means the robotic snake can not only make quick movement response, but also keep the body supple. To test this hypothesis, a tensegrity robot has been constructed and the ability of the snake-like robot to complete different actions on a range of terrains, as described in Chapter 5, has been studied. Details about the mechanical structure and control of the prototype are discussed in Chapter 3 and Chapter 4.

Throughout the project period, the research followed several changes in the specific tensegrity structure chosen to imitate the tension network of the snake. Initially, a range

of existing tensegrity structures were investigated. However, upon further consideration, these were deemed impractical due to the fact that those tensegrity structures in the existing studies were relatively bulky or inefficient in motion. Therefore, in order to design a tensegrity snake-like robot that can actually move, attention must be paid to its actual installation. Its design needs to be as simple as possible, to avoid the overstuffed assembly.

The final structure chosen then became a a simplified version of the standard tensegrity structure. According to the principle of snaking movement, some combinations of motors and ropes were replaced by a spring to spare installation space and save energy.

1.2 Thesis Structure

Chapter 2 provides an overview of the literature relevant to this thesis, specifically different types of snake-like robots, as well as the bionic properties of tensegrity structures. Also in Chapter 2, tensegrity structures are compared in detail with some traditional structures. Chapter 3 is a complete introduction to prototype design and motion analysis, describing how to simulate some movement of snakes in theory. Chapter 4 provides complete hardware details and control details about the prototype, including the materials of each part of the prototype, software platform, control program, control mode and so on. Chapter 5 details the prototype experiments in terms of content and results. Chapter 6 concludes the thesis with a discussion of the potential of using tensegrity structures to build robotic snakes based on the experiments.

2 Literature Review

A literature review is undertaken to investigate the potentials and methods of using tensegrity structures to build a robotic snake. It includes the characteristics of snake locomotion, a review of existing robotic snakes and their potential applications, the development history and the control methods of tensegrity structure and the current researches on the snake-like robot with tensegrity structure.

2.1 The Characteristics of Snake Locomotion

In nature, snakes have a rich and unique way of locomotion and can adapt to different terrains, such as deserts, forests, cliffs and rivers. Generally speaking, there are four common ways for snakes to move [31]:

1. Concertina
2. Serpentine
3. Sidewinding
4. Rectilinear

Fig.1 shows these four movements. Snakeskin also has remarkable surface properties, making their movements more efficient.

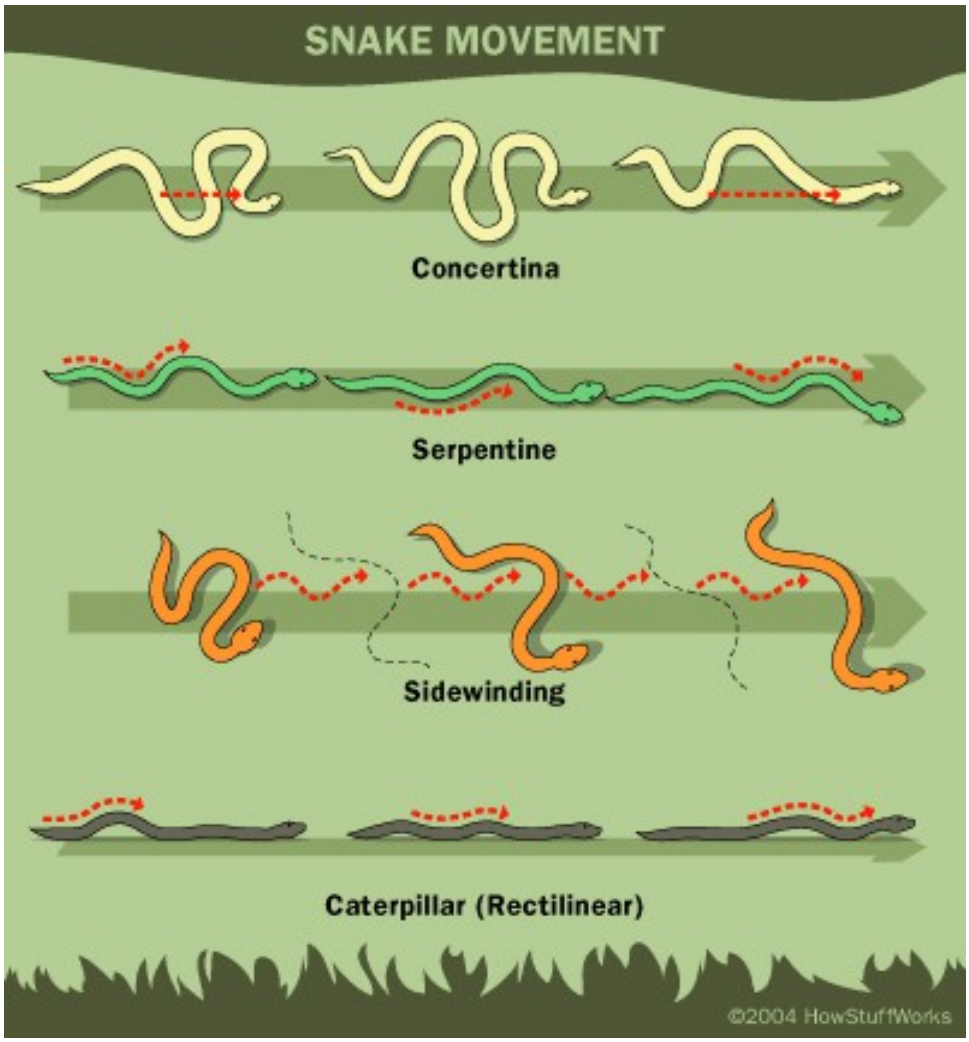

Figure 1: Four common ways for snakes to move (taken from [11])

2.1.1 Concertina

Concertina movement, is often seen in spatially confined environments, such as tunnels. This movement eliminates the need for a lot of space which is required in serpentine (lateral undulation) and sidewinding (lateral circling). The snake can bend its body so that a part of itself is pressed down on the tunnel to form a relatively fixed anchor point, and then push its body forward alternately. This motion is slower than serpentine and sidewinding, but can still reach 10 percent of the snake's length per second.

Typical concertina movement is shown in Fig.2.

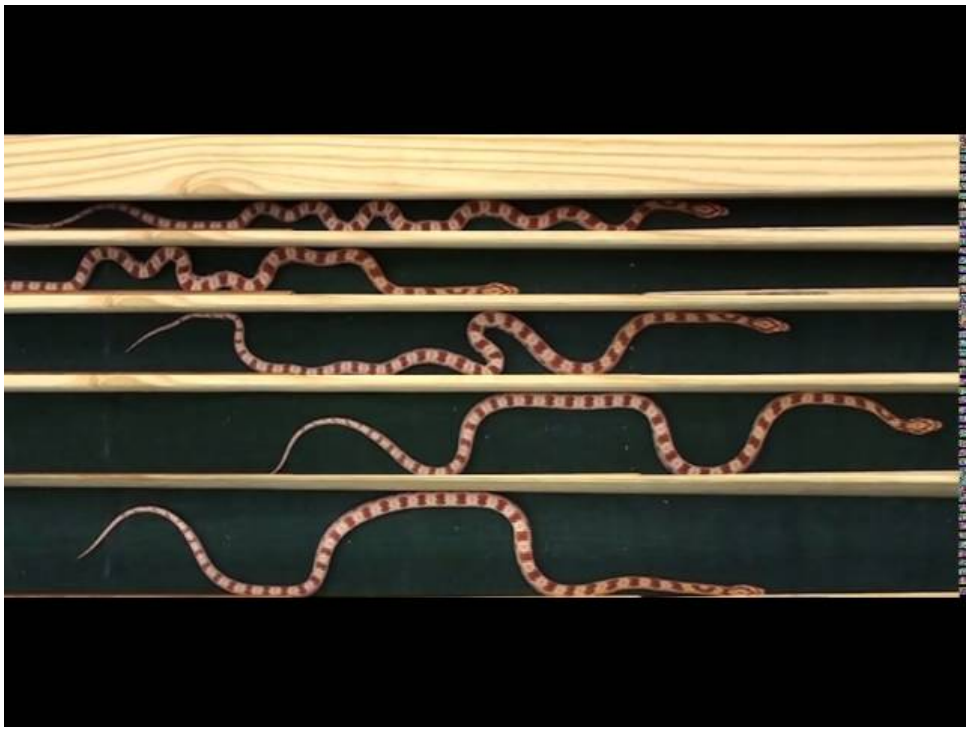

Figure 2: Schematic diagram showing concertina movement of a snake in confined channels (taken from [28])

2.1.2 Serpentine (Lateral Undulation)

Serpentine (lateral undulation [51]), the most common form of locomotion used by most snakes on land, has the same energy efficiency as running with the same mass by lizards. In this mode, the snake's body alternately bends to the left and right, creating a horizontal wave [17] that travels backwards in motion. Each joint of the body gets a counterforce to the surrounding environment and the whole body gets a resultant force in the midline thrust to move forward, while the lateral components of the counterforce cancel each other out. In this mode, each point of the snake's body follows the path of the previous point, so this mode allows the snake to move through thick vegetation and

narrow gaps. Also, lateral undulation is the only mode that snakes can move through the water. But because the friction on the ground are different, snakes need different muscle control ways to move laterally between in water and on land. Typical serpentine movement is shown in Fig.3.

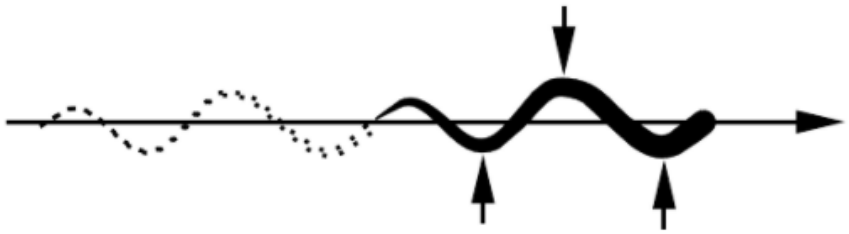

Figure 3: Schematic diagram showing serpentine movement of a snake (taken from [39]) (The long arrow indicates the direction of the movement, and the small arrows mark the left and right poles of the path.)

2.1.3 Sidewinding

Sidewinding, an improved version of lateral undulation, costs only two-thirds as much energy as running with the same mass by lizards. In sidewinding, one part of the snake stays in contact with the ground in the same direction, and the other part is lifted from the ground, so snakes can alternately use one part of their body to roll the other to achieve a state similar to rolling sideways on the ground. This movement greatly overcomes the snake's slippage on sand or muddy ground. Typical sidewinding movement is shown in Fig.4.

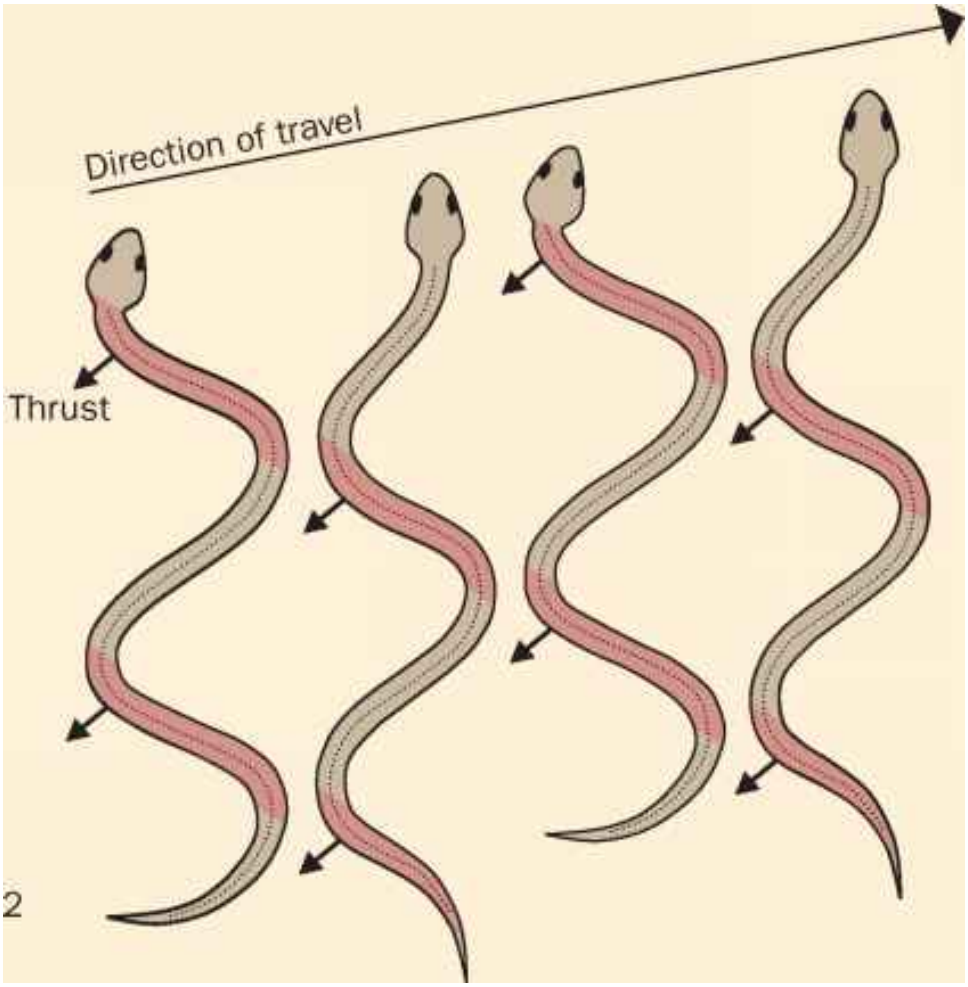

Figure 4: Schematic diagram showing Sidewinding movement of a snake (taken from [14]) (The red parts indicate that they are in contact with the ground. The snake keeps rolling over the other parts, but the part that is in contact with the ground always remains a line segment in the same direction, allowing the snake to keep rolling.)

2.1.4 Rectilinear (”Caterpillar”)

Rectilinear, the principle is similar to caterpillar motion [37]. By moving in this way, the snake doesn’t have to bend its body horizontally unless it needs to turn directions. In this mode of locomotion, the snake moves forward through the subcostal muscles, the costal muscles, and the skin while the ribs do not move. The subcostal muscle and the

costal muscle connect the ribs to the skin. The costal muscle can pull up a portion of the snake's abdomen from the ground and place it in its front position. As the scales of the abdomen stabilize on the ground, it can lift the back ribs off the ground and place them in a more forward position. This creates a series of backward ripples in the snake's body, with the peaks rising off the ground and the troughs falling to the ground, alternating with each other.

It is not difficult to find that the speed of rectilinear movement is not high (between 0.01 and 0.06 m/s). But it also has significant advantages. First, it's almost noiseless and hard to detect. Second, it doesn't require a lot of space to move around, so it's good for moving through narrow spaces. It is also worth noting that this movement requires less spinal curvature which means the body movements is small. Because snakes can switch the marching strategy easily, so rectilinear movement is often combined with other movements. For example, when climbing, snakes usually combine rectilinear motion with concertina motion. Typical rectilinear movement is shown in Fig.5 [27].

Figure 5: Schematic diagram showing Rectilinear movement of a snake (taken from [27]) (The blue parts indicate that they are in contact with the ground.)

2.1.5 Comparison of Movement Modes

In addition to regular ground movements, they can also perform special climbing, such as moving from branch to branch. However, it is relatively slow and complex, which is

beyond the scope of this project.

Through a comprehensive comparison of the above four common snake movement modes, it can be found that rectilinear movement has a relatively low efficiency of action, which has a lot to do with the friction of the contact surface [32], but also it is effective on a range of environments. The serpentine (lateral undulating) motion is a conventional motion mode, which is suitable for general natural environment and takes into account both speed and energy loss. However, serpentine motion requires more freedom to undulate from side to side, which can be limited in certain environments (such as small caves), and effective serpentine motion requires sufficient body length and a reasonable amount of weight [12]. Therefore, the design of the snake robot in this project will be based on the rectilinear motion, and then consider to realize the serpentine movement (more factors to consider), so as to achieve a balance between robustness and motion efficiency.

2.1.6 Snakeskin features

Snakeskin has unique friction properties. The skin has the least friction when the snake slides forward. As the snake slides laterally, the coefficient of friction doubles. When the snake slides back, the coefficient of friction is quadrupled [33]. By adjusting the muscles in the abdomen, the snake can control the torsion stiffness of body, thus affecting the scales on the ventral side. This degree of freedom for friction control allows the snake to effectively handle interactions with the complex environment and save energy [33].

Therefore, in addition to regular muscle control, the control of snake scales on fric-

tion also affects the efficiency of snake movement, which is also worth researching for snake-like robots. For instance, in 2018, Tung D. Ta et al. proposed a printable directional friction layer to support peristaltic soft-bodied robots [46], as shown in Fig.6.

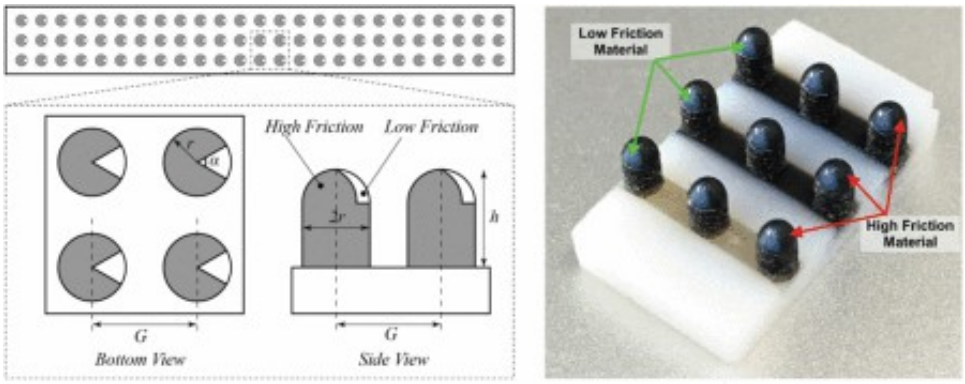

(a) Ventral surface of the robot is divided into circular regions of radius r, the gap between two consecutive circular regions is G. Shaded part is high friction material, low friction material (white part) occupies a part of each region at angle α. From side view, each circular region is a rounded cylinder of height h.

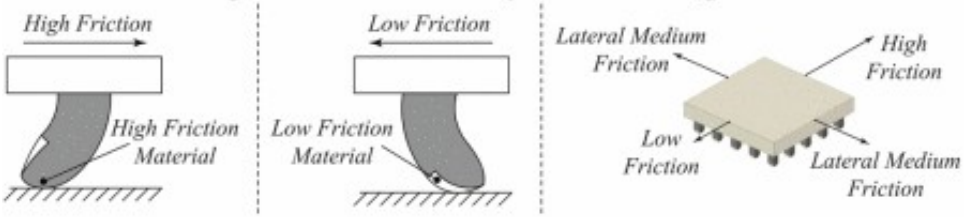

(b) Bending of the rounded cylinder will make the whole surface frictional anisotropy

(c) Low friction forward

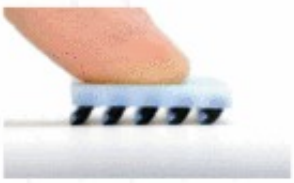

(d) High friction backward

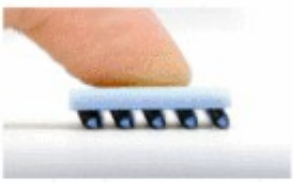

(e) High friction laterally

Figure 6: A printable directional friction layer (taken from [46])

2.2 The Characteristics of Robotic Snakes

Robot is known as a machine which is capable of executing tasks automatically. In today's society, robots have been popularized to serve human beings, such as some dangerous tasks, highly repetitive tasks or work in environments unsuitable for human existence.

Among them, robotic snakes are often designed for special missions in extreme environments, including extraterrestrial surface exploration, earthquake rescue and so on. There are several possible reasons for this choice. Firstly, the snake-like robot is the result of biological inspiration, which enables the snake-like robot to imitate the movement of the snake, namely, the movement without limbs. So it allows the robot to maintain a low center of gravity, making the robot easy to achieve robust control. Meanwhile, Robotic snakes can move in the environment such as lawn, forest and sand with only the friction force of the body which also makes mobility safer (not susceptible to impact, and not easy to bump into people and objects) and more invisible (no environmental noise, no attraction to animals), to help robots better complete rescue and exploration missions. Secondly, the narrow feature of the snake-like robot makes it easier to pass through general obstacles. And one thing that can't be ignored is that the small snake-like structure can make full use of the body's freedom to perform many specified movements. In a sense, this represents the potential to accomplish complex tasks.

The special structure and control mode gives the robotic snake different application fields from the traditional robot. Using the redundancy of joint movement of the robotic snake can make its head maintain a specific posture [47], which is convenient

for the robot to carry sensors and cameras [40]. By using sensors such as ultrasonic sensors and PIR (Passive Infrared Ray) sensors, robotic snakes can gain a sense of the surrounding environment, build maps and navigate [7], helping detect places that are difficult for humans to reach or dangerous. They have considerable potential in search and rescue work. Some robotic snake is used in earthquake relief, and it can achieve better results in cooperation with other robots [19]. It is worth mentioning that the snake robot is also suitable for underwater missions [41], as shown in Fig.7 [41].

Figure 7: Underwater swimming manipulator (taken from [41])

Therefore, although the snake robot has a more complex mechanical structure than the common wheeled robot and requires higher control requirements, it is still one of the research hotspots due to its characteristics that allow it to perform more diverse tasks.

2.3 Different Kinds of Snake Robots

Since 1972, robotic snakes have been researched with the goal of achieving mobility on a variety of challenging terrains. The first generation of snake robots, ACMIII [20],

as shown in the Fig.8, its body is in contact with the ground through wheels and swing from side to side by relying on the servo motor at the joint. The original series of this snake-like robot had limited degrees of freedom and could move only on flat surfaces. In 2001, ACM-R3 [36], as an improved version of ACMIII was able to perform three-dimensional movements and effectively simulate many of the snake's actions, as shown in the Fig.9.

Figure 8: ACM prototype (taken from [20])

Figure 9: ACM-R3 prototype (taken from [20])

There have been a number of studies of robotic snakes similar to ACM structures, which twist the robot's body by means of rotatable joints connected to the body, and some of them add wheels underneath the body to control friction. This type of robotic snake has some differences in the structure of the rotating joints. A series of explorations have been made on the structure and motion control of robotic snakes.

In 1993, Y. Shan et al. designed a simple, wheeled, snake-like robot consisting of articulated chain joints, each with an electric motor and a linear solenoid. The simple motion plan allows the robot not to avoid obstacles on its way, but to continue to move toward the target as it comes into contact with them. The snake-like motion features allow the robot to continue to move, while the robot keeps pushing against the obstacles [44].

In 1999, Shugen MA had a research which discussed the muscular force for the uniform locomotive curve [31], and also compared the locomotive efficiencies for various creeping movement curves of snake locomotion, by analyzing the ratio of the tangential force to the normal force and the power required for snake locomotion. It proposed a new Serpentine curve which resembles the actual form of the snake in shape and shows the highest locomotive efficiency, and thus is more valid as a snake creeping locomotion shape than the Clothoid spiral, the Serpenoid curve, and others.

In 2007,an article from Sang-Jin Oh et al. presented an omni-tread snake robot [38], Caleb III, as shown in Fig.10, that is designed to locomote in narrow space and rough terrain. They compare the real robot's experimental results with the simulation results in the case of a straight line motion, a right turn motion and a left turn motion. This is a fully-tracked snake-like robot, which relies on the crawler on the joint to complete

forward movement and can turn left and right together with the rotating joint. It mainly imitates the shape of snake movement, but its movement mode is still very different from that of the snake.

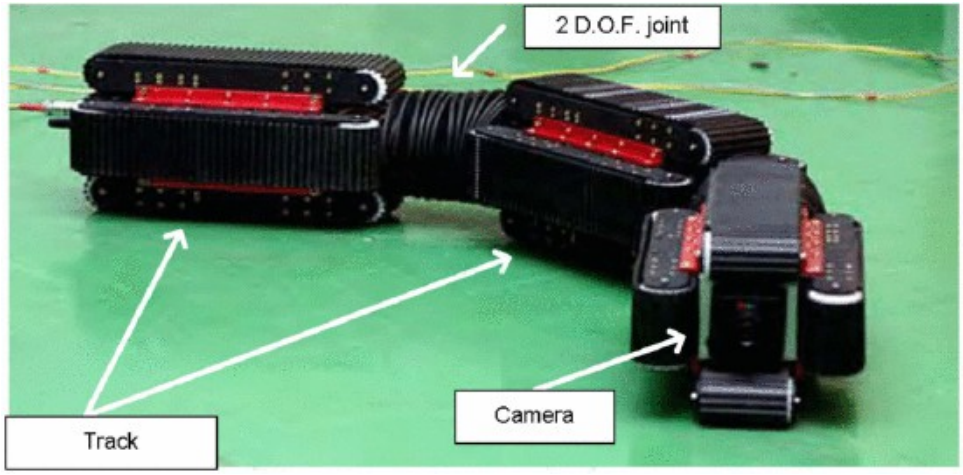

Figure 10: Caleb III (taken from [38])

In 2008, the paper published by J. Sitár et al. dealt with mechanical construction, basic design, simulation of designed structure and final realization of a combined snake-like robot [22], as shown in Fig.11. Designed and simulated model is finally realized from lightweight materials mainly from duralumin and nylon. This robotic snake uses a special rigid joint connection to realize the omnidirectional rotation between joints. Objectively, it can simulate any movement of snakes and can adapt to a variety of terrain, but the movement speed is slow and the joints are complex and bloated, making it difficult to miniaturize.

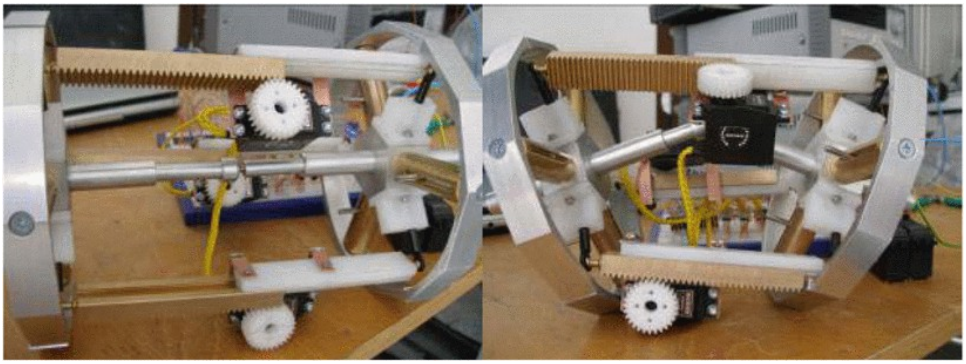

Figure 11: Prototype built by duralumin and nylon (taken from [22])

In the same year, Ahmadreza Rezaei et al. researched and realized a snake-like robot with joints made of elastic rubber and ropes between each adjacent segment, as shown in Fig.12. The robot moves along a sinusoidal curve. This control mode is similar to a simple soft snake-like robot, which makes the whole body form a sinusoidal waveform and uses friction force to push itself. The disadvantage is that it is not particularly flexible and just has one single movement mode, which makes it difficult to perform some delicate actions. [42]

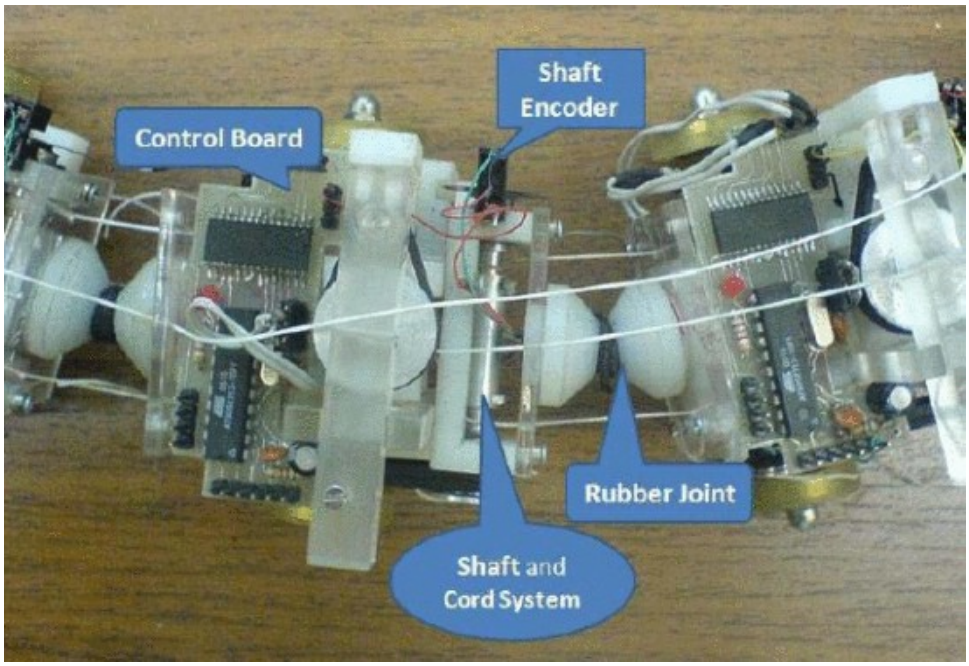

Figure 12: A snake-like robot made of elastic rubber and ropes (taken from [42])

In 2010, Xiaofeng Ye et al. presented the design and implementation of a novel modular snake robot [52] for rough terrain, as shown in Fig.13. The joints of the snake-like robot allow it to rotate up and down. Using this, the snake-like robot squirms forward as a cosine function that undulates through space, changing the direction of squirming by changing the period of the created cosine function. The snake-like robot can traverse over obstacles that are lower than its segment is, and its maximum speed is limited by frequency and amplitude of the path(the sine wave) that the body follows when moving. When the frequency is too high, the joint will have difficulty rotating.

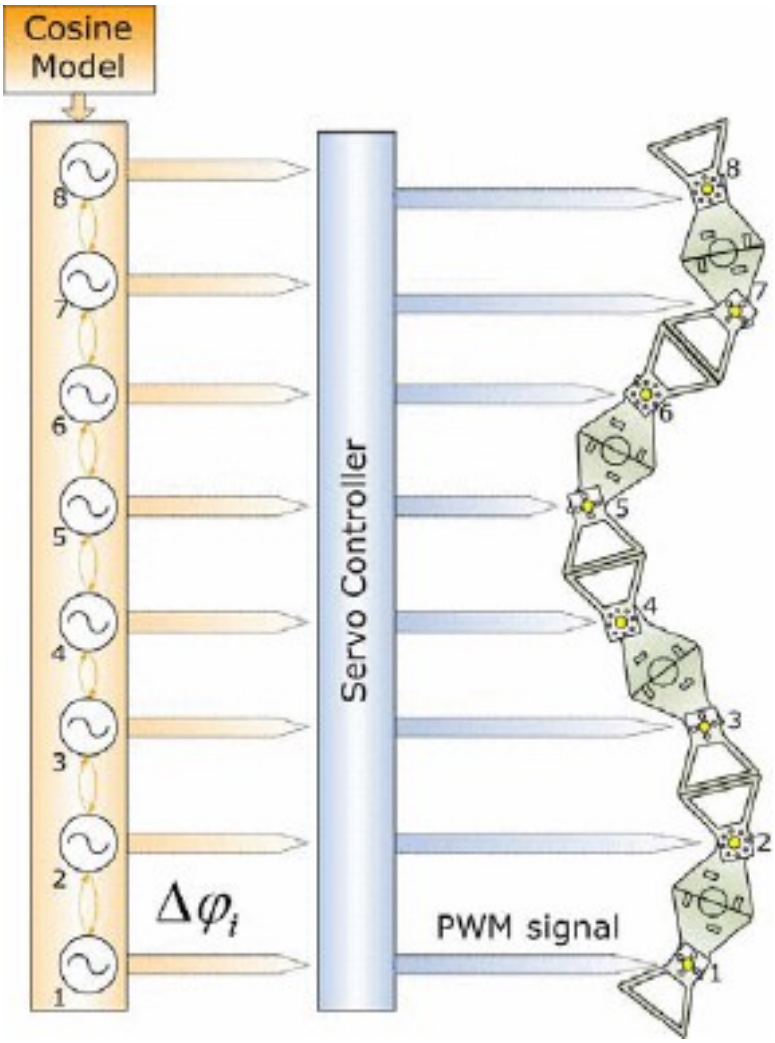

Figure 13: A novel modular snake robot (taken from [52])

In 2011, Thanniti Khunnithiwarawat et al. had a research which aims to study the locomotion of a wheel snake robot MOMO [26] in different environments, as shown in Fig.14. This snake-like robot can rotate its joints up, down, left, and right, while each body has drive wheels to help it move. In the forward gait attempt, MOMO has tried three modes of sinusoidal gait, namely, drive wheel and joint under asynchronous control, joint using sinusoidal motion with passive wheel, and active wheels using a sinusoidal gait. In this work they experimented with three types of environment: a

flat ground, a slope and a tight corner. The experiment shows that the Active-Wheel Sinusoidal (AWS) gait is the best solution for traveling on a flat ground and a slope.

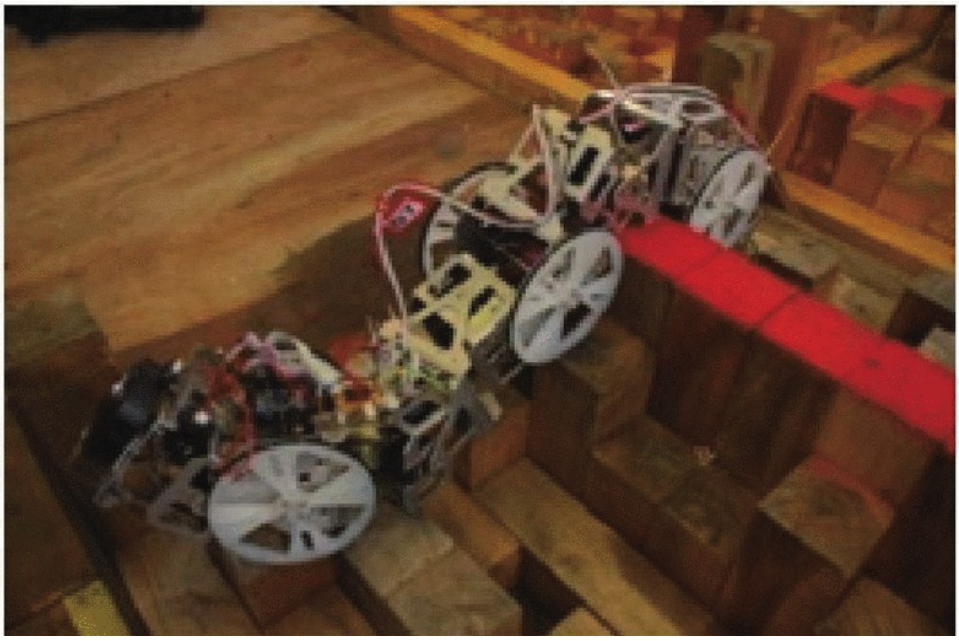

Figure 14: MoMo (taken from [26])

In 2016, Sajjad Manzoor and Youngjin Choi had a design concept of new modular snake robot [43]——It is constructed by joining a number of similar modules and each module in the body has three degrees-of-freedom, as shown in Fig.15. In addition an active prismatic joint is provided inside each body module to achieve rectilinear motion along the body of snake robot. In terms of the rich degree of freedom between the joints, it is enough to simulate all types of snake movement on the ground. It also has body modules, a neck module, a tail module and a head module, mimicing the form of a snake.

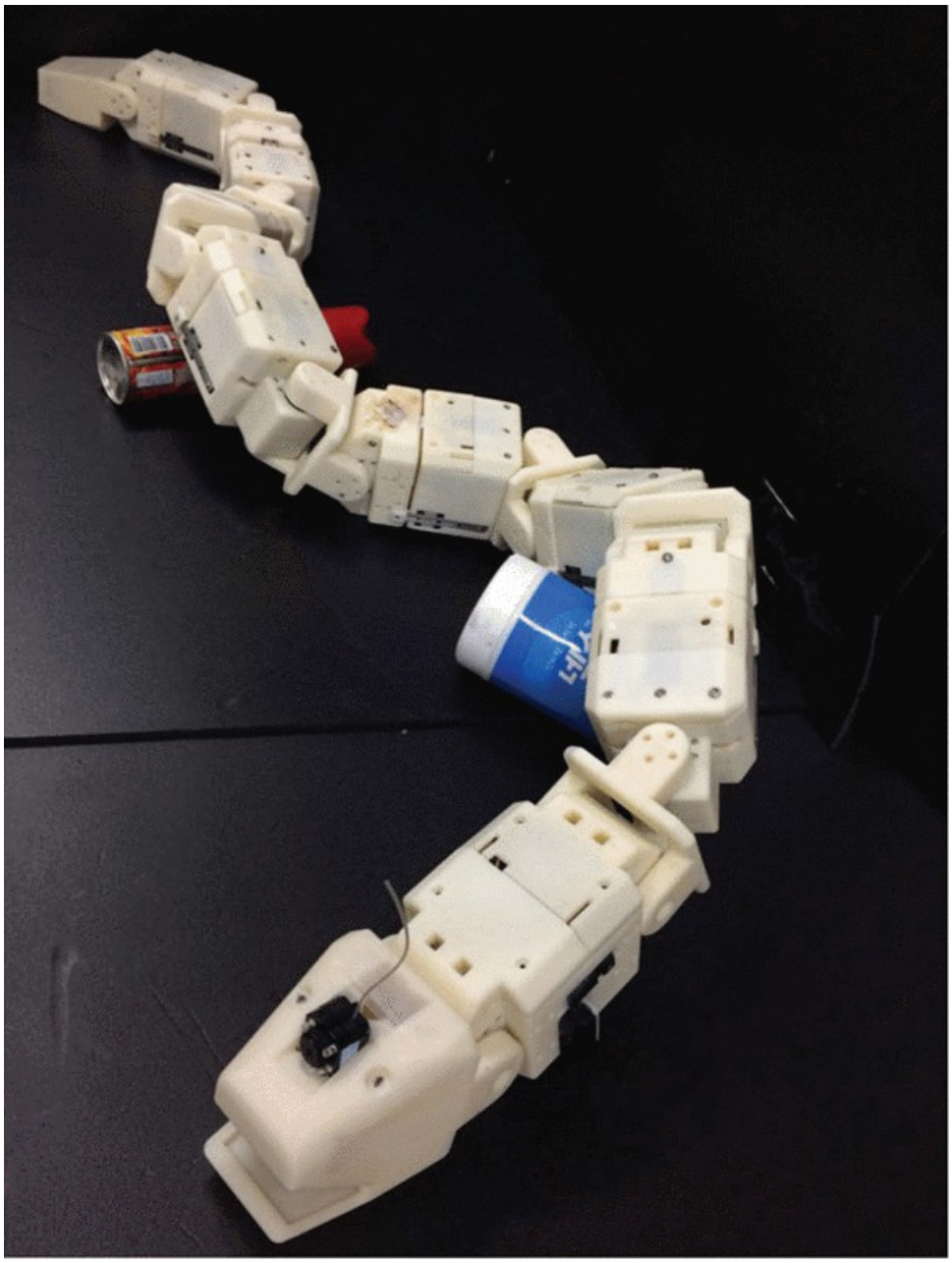

Figure 15: A new modular snake robot (taken from [43])

In 2017, Callie Branyan et al. presented an entirely soft snake robot [5] designed to implement the prerequisite shape space for slithering gaits, as shown in Fig.16. It is a modular two-chain soft robot that uses a geometric mechanical model to guide control strategies and employs several cyclic gait patterns to generate forward displacement.

This robot mimics the lateral undulation.

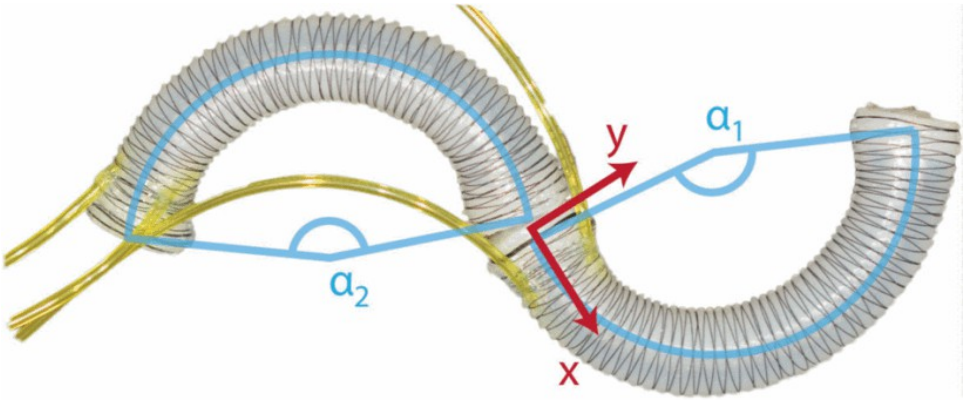

Figure 16: An entirely soft snake robot (taken from [5])

In 2018, Lei Tang et al. completed simulations and experiments about the motion of cable-driven snake robots [48]. As shown in Fig.17, they glide the snake-like robot along the planning curve, which greatly reduces the size of the motion plan and effectively solves the problem that inverse kinematics and control become more and more complex when the serpentine robot has redundant degrees of freedom.

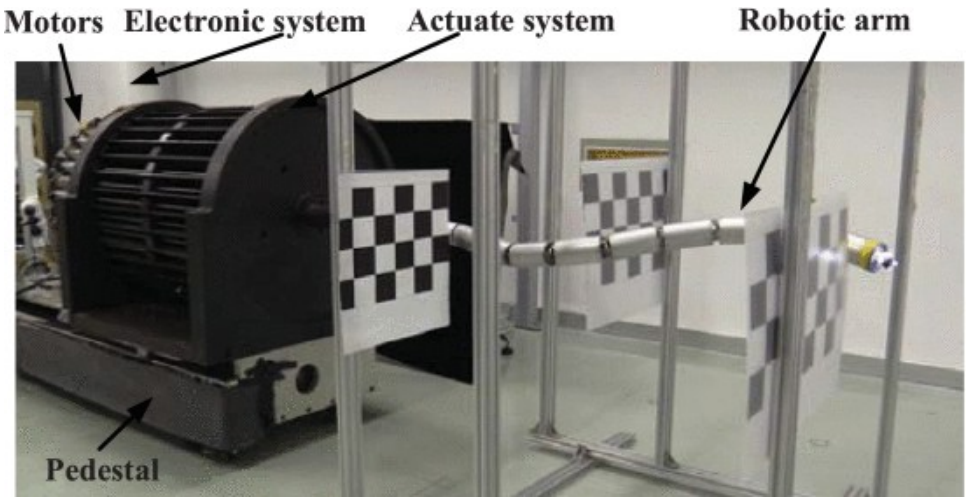

Figure 17: Experiments about the motion of cable-driven snake robots (taken from [48])

In 2018, Atsushi Kakogawa et al. proposed an N-link snake robot with parallel

elastic actuators (PEA) [24], and added springs to its joints, as shown in Fig.18. A typical snake-like robot uses motors to drive joint rotation, which consumes a lot of energy in rapid response. By adding PEA into the original structure, although the spring prevents joint motion, when the required motion of the joint is periodic, the torque and power required for the motion can be greatly reduced by synchronizing the actuator output (rotating joint) with the spring resonance frequency. With proper control, the addition of springs can greatly enhance the gait of the snake-like robot.

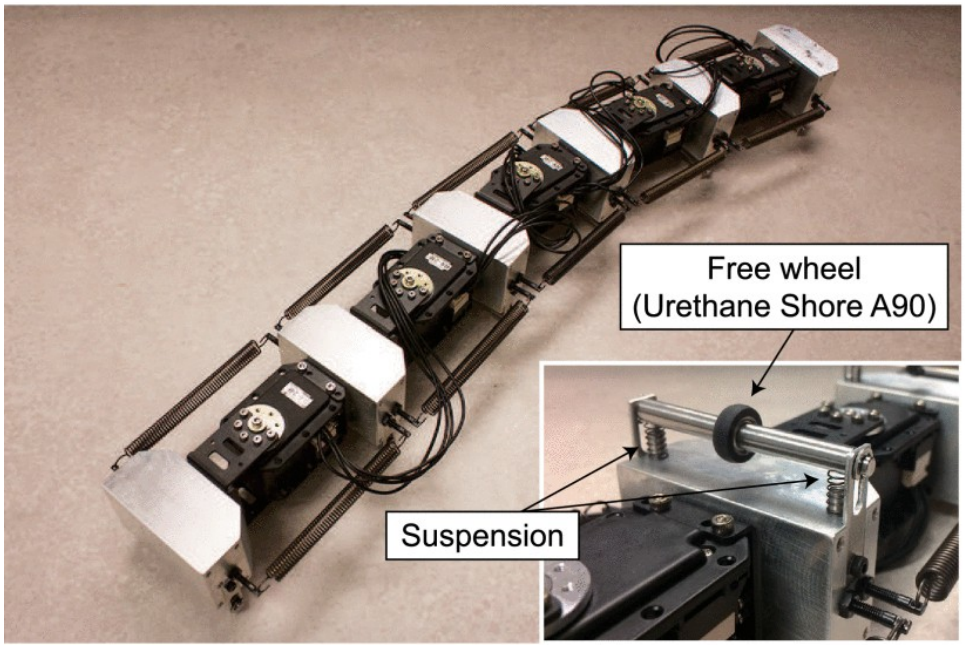

Figure 18: An N-link snake robot with parallel elastic actuators (taken from [24])

In generations of snake-like robots, researchers have focused on how to mimic the overall movement of the snake's body. Given the mechanical structure of the robot, this is easy to understand. The rigid structure can only simulate the distortion of the body, just as the spine of a snake, which relies on nodes of the spine to deflect the body, without the function of the muscles.

Soft robots, on the other hand, have no clear body contortion nodes. Compared

with rigid structures, they can make more flexible and compliant movements, but their motion efficiency will be reduced. In addition, due to control mode limitations [5], the soft robot snake is generally limited to several action modes, so it will also have some difficulties in fine control.

There are also cases where rigid structures are combined with flexible materials, such as cable-driven snake robots [48]. These still have a rigid structure in the joint connection, but it rotates not through servo motors but through changes in the tension of the cables on both sides, which makes the robot move more smoothly and distributes the torque required to rotate the joint. It is the tensegrity robot that uses the change of tension to change balance inside the structure and shape of the robot.

2.4 Tensegrity Structure

Tensegrity is a concept that extends from architecture, a portmanteau of 'tensional integrity' which describes rigid compression elements held in place entirely by the tension of flexible members.

Many architectural and natural phenomena are considered to conform to the idea of tensegrity, but there is no consistent and clear definition to demonstrate the definition of tensegrity. In general, a structure consisting of isolated members (sticks, struts) through a network of strained tension (cables, tendons) is considered to be a tensegrity structure [23].

An effective tensegrity would have been unthinkable before the 18th century because there were no suitable materials to support the tension in the structure. But with the progress of the times, the appearance of new materials gives people the chance to

imagine and design. Mass production of materials with both compression and traction reaching 50,000 PSI began in 1851, leading to the construction of the Brooklyn Bridge, which ushered in an era of innovation in tension design. Before that, the first suspension Bridges were made of rope and wood, invented many centuries ago, and although they were also based on the concept of tension structures, their load-bearing capacity could not support heavy loads. Therefore, the innovation of materials is crucial to the future of prestressed structures, whose compression members must be more resistant to buckling, and whose tensioned members must be more resistant to traction.

Although the tensegrity theory was established relatively late, the design of tensegrity is constantly emerging because it can create a variety of portable and adaptable shapes. Kenneth Snelson, considered the pioneer of minimalism, created tension-based sculptures for international exhibitions as early as 1948. He has some designed tension-based structures like the double-hulled dome [45]. In the mean time, he tried a lot of structures and materials, trying to analyze the efficiency of different tensegrity structures. He used weaving to obtain the inspiration for the internal connections of tensegrity structures, and the rich organization of tensegrity structures allowed him to imitate many other structures and expand freely on the existing ones.

Since the 1960s, many engineers and architects have joined the field to design tensegrity structures. Many tensegrity structure designs have been put to practical use, such as “vector equilibrium” (cubo-octahedron), the “thirty-islanded Tensegrity sphere” (icosahedron), the “six-islanded Tensegrity tetrahedron” (truncated tetrahedron) and the “three-islanded octa-Tensegrity” [23]. In this period, people mainly paid attention to the tensegrity structure because it conforms to the connotation of minimalism and has

a strong sense of design. Many people thought that tensegrity structure belongs to the category of engineering research.

In the 1980s, many people began to expand on previous studies, and began to study tensegrity structures more deeply from the perspectives of geometry and mathematics, in an attempt to study tensegrity systems more systematically. The goal of Connelly and Back was to find a suitable three-dimensional generalization for tensegrity structures [10]. Using the mathematical tools of group and presentation theory and the capabilities of computers, they mapped out a complete catalogue of tensegrity structures, specifying in detail the types of stability and symmetry in tensegrity structures.

However, the connotation of tensegrity is not limited to the field of architecture, people generally begin to think that tension structure itself is ubiquitous in nature and the universe. Ingber [21] found that not only cells, but also a variety of natural systems are constructed according to the Tensegral model: carbon atoms, water molecules, proteins, viruses, tissues and other organisms. Meyers [34][8] used tensegrity to explain the relationship between animal and human muscles, tendons and bones. They claimed that the skeleton is not just a framework for supporting muscles, ligaments and tendons, but a set of compression components suspended in a network of continuous tension.

Considering this way of maintaining the structure of objects through tension can adapt to many extreme environments, part of the robot structure design also contains the concept of the tensegrity structure. An application called the SUPERball has been researched in some space exploration plan. This kind of robot structure, which relies

entirely on bars and cables, has many advantages: self-deformation, foldability and lightweight [30].

From the perspective of bionics, the traditional tensegrity structure is very similar to the musculoskeletal system of organisms. The bones play a supporting role, while the tension and relaxation of multiple muscles drive and restrain the movement of the bones. The advantages of this mode are obvious. Firstly, it can keep the structure in a tense state and maintain pre-tension, so that the robot can respond to actions more quickly. Secondly, the structure can disperse the impact received by slight deformation, while the torque required for movement will be distributed among multiple tendons (cables) [3], making the movement more robust [35]. Finally, the structure is very light, and shows rich degrees of freedom through changes in tension [15]. This structure with rich degrees of freedom also puts forward higher requirements for the control mode [2].

2.5 Tensegrity Robot Control

The introduction of tensegrity structures from architecture and art to robotics means that the influence of tension changes in structures needs to be considered. When a robot goes from one state to another, it needs to change the tension through the control device to complete the transition from one stable static state to another. How the specific tension structure is designed, and how the tendon is controlled, determine how the robot is controlled. Common tendon materials used to connect joints include twisted string actuators, pulleys, springs, flexinol muscle wire, nitinol smart metal, etc. Depending on the connection material, the researchers used different control methods. The following are some of the more common control methods.

Fully Actuated Using Twisted String Actuators: Structures that can use twisted string actuators for all tension members are very common, for example: the six-strut tensegrity [13] (as shown in Fig.19). The advantages of using twisted string actuators are very obvious, for researchers can directly control the tension at each joint, the line length, and achieve multi-degree of freedom motion through the combination of tensions. However, it also has obvious defects. Multiple motors make the structure heavier and larger volume, and the robot's movement efficiency is not high while the cost is high due to its complete dependence on the motors at each joint.

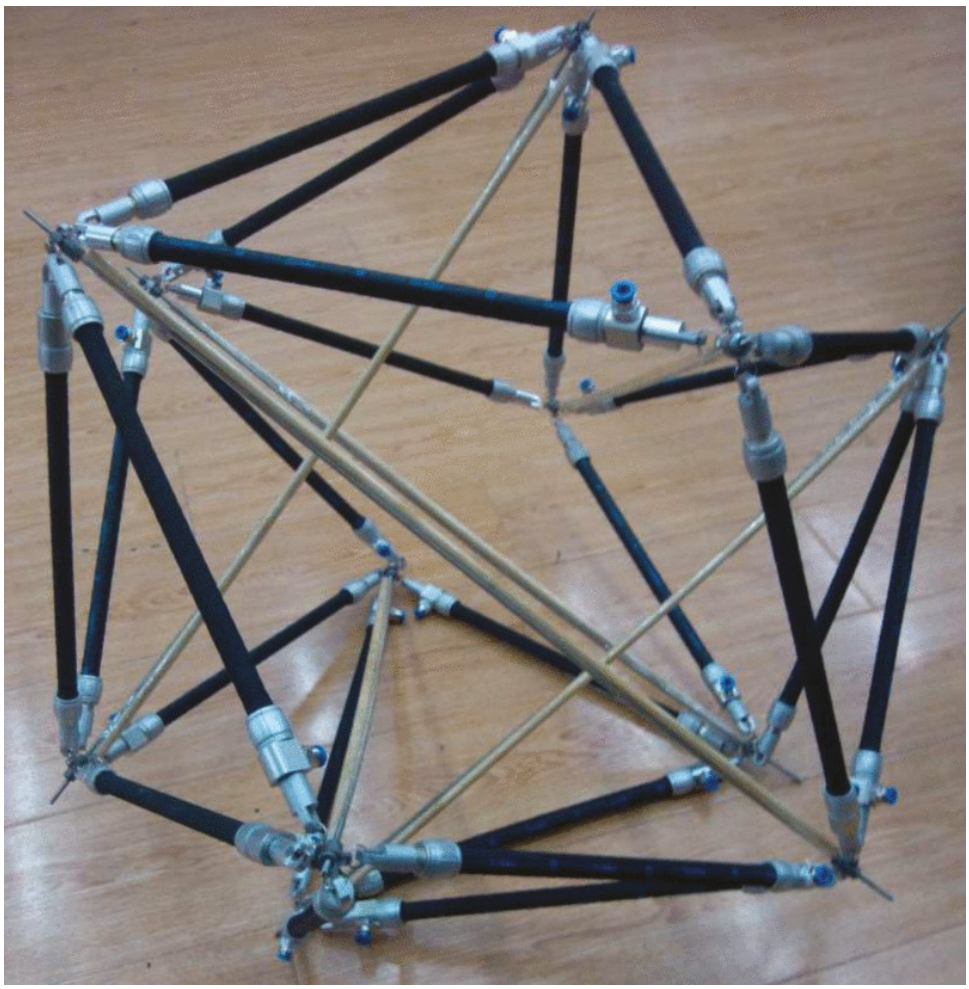

Figure 19: Six-strut tensegrity (taken from [13])

Pulley Actuation: The use of pulleys gives the motor more freedom to position itself, and it can help to reduce the torque applied by the motor to the structure through rich and diverse designs [3] (as shown in Fig.21). The drawback is that more space is needed for the pulley to be used and lower drive ratios are possible.

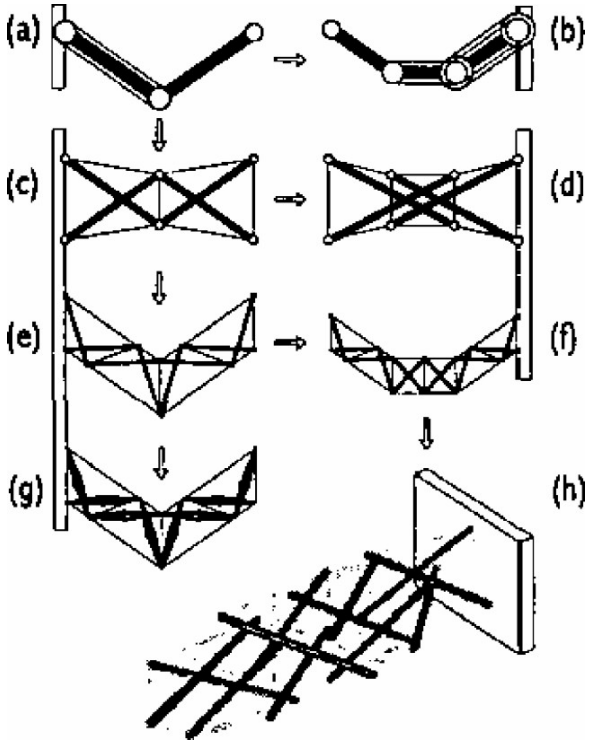

Figure 20: An illustration of a simple rigid structure transformed by a tension network. (taken from [3]) (It is not difficult to find that the torque required by the original structure can be effectively dispersed through the tension network.)

Local Addition of a Spring: Springs are a very good energy storage element, and when the motion can reach the same frequency as the spring oscillation, they are able to improve the motion efficiency of the mechanism, and reduce the energy loss [24].

2.6 Research on Robotic Snakes in Tensegrity

In the last ten years, the research on robotic snakes with tensegrity structures is still in the stage of theoretical analysis and simulation. There are few cases in which these designs can be realised and the robots can be put into use.

In 2006, J. B. Aldrich and R. E. Skelton proposed to build a snake-like robot (as shown in Fig.21) using electric pulleys as tendons to drive tension networks [2], and they minimized motor torque through a position-feedback motion control rule, while ensuring that the tendon does not slacken as it moves along a specified trajectory. However, there are some problems in the implementation, one is that the mechanical structure envisaged is difficult to achieve, the other is that the control mode is still not reliable enough.

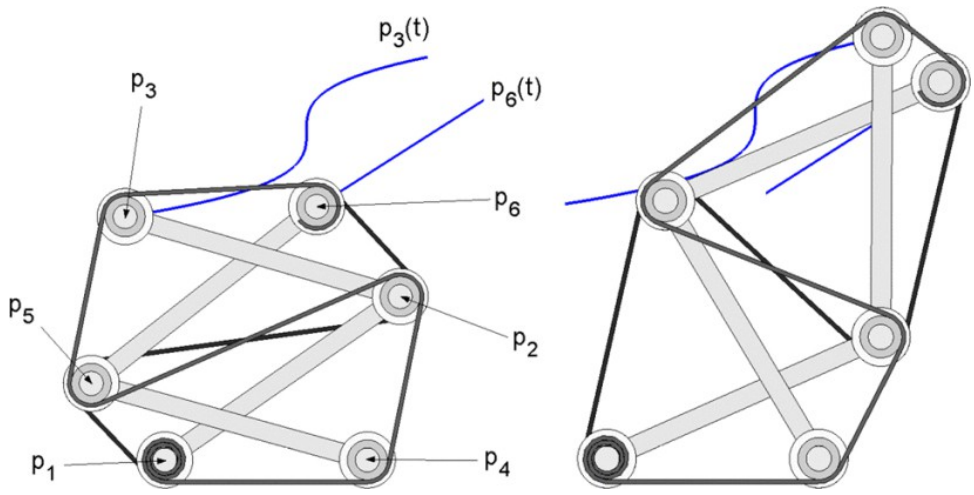

Figure 21: Tension networks that require more free space (taken from [2])

The envisaged mechanical structure requires no sliding friction between pulley and pulley in order to meet the current stability and subsequent control. Generally, this needs to be realized by a device similar to bicycle chain, which leads to the fact that

the envisaged physical mechanism requires complex component combination, which increases the difficulty of implementation.

In terms of the control method, although the author proposed the control method based on the position feedback motion control rule, there are still problems in the actual use. Firstly, this control method requires a lot of computation, and with the increase in the number of joints, the computation will increase a lot. And the model itself has a high requirement on the control. It has only through two tendons achieve a network of tension, the advance needs to consider how to keep the network before the movement of the tension, tension moment need precise changes in the movement to ensure that the tendon tightens, so higher control ability is needed to form movement inertia to help stabilize the tension structure, in the meanwhile, to complete the goal. The demanding mechanical structure and control make it difficult for the supposed snake-like robot to be built into real objects.

In 2013, Brian R. Tietz et al. developed a modular tension robot inspired by the spine called Tetraspine [49], as shown in Fig.22. The robot was made of a rigid tetrahedron with six stringy joints. The model was simplified based on the spine designed by Tom Flemons (as shown in Fig.23), which requires eight strings to connect. With this simplification, the robot has more surface area for motors, controllers and sensors, and the tetrahedron can better touch the ground. In the simulation, the structure was tested on flat ground, steering and irregular ground. And then finally in the physical validation phase, it can be seen that the physical objects of the model are still very bloated – six strings are needed for a joint, in other words, six motors are needed to control the tension. Due to its bulkiness (deviates from the theoretical model), the prototype had

difficulty moving as smoothly as expected with only two modules.

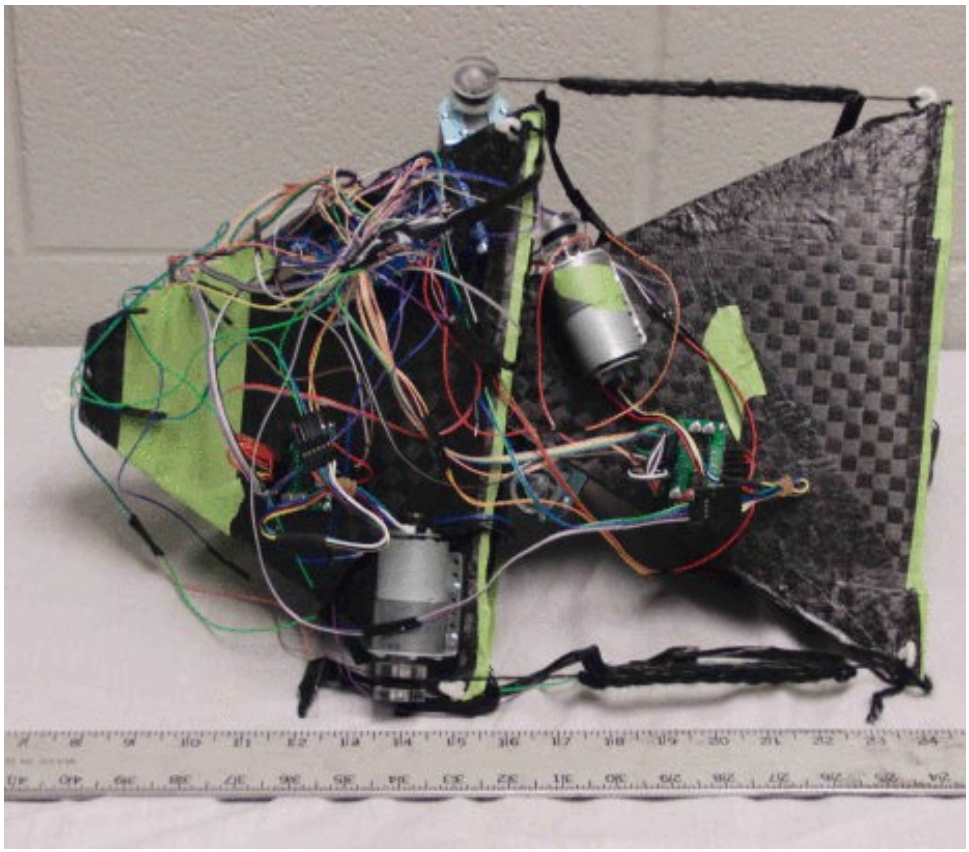

Figure 22: Tetraspine (taken from [49])

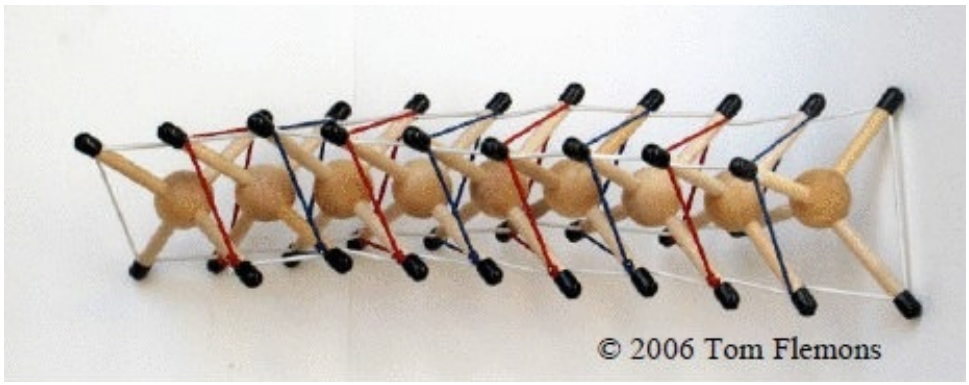

Figure 23: The spine designed by Tom Flemons (taken from [49])

Therefore, although the design of a tensegrity structure is relatively simple, supporting mechanical equipment and electronic components can easily make the robot

structure bloated, and the tensegrity structure needs a large free space to meet the change of the overall structure caused by the tension. Hence a reasonable tensegrity structure is the basis for good experiments, and the key is to simplify the tensegrity structure so that the snake-like robot can move efficiently.

In 2018, Francisco Carreno and Mark A. Post studied a prototype that uses a tensegrity structure to travel air ducts [6]. This wheeled tensegrity robot (as shown in Fig.24) provides a good idea - it may be more appropriate to use a tension network to connect various rigid structures for practical applications, because such a hybrid structure can obtain the advantages of a tension network: stability, easy adjustment, low cost, and also gives consideration to the efficiency of robot work. From this point of view, the robotic snake designed in this project is also considered to combine the rigid structure and tensegrity structure.

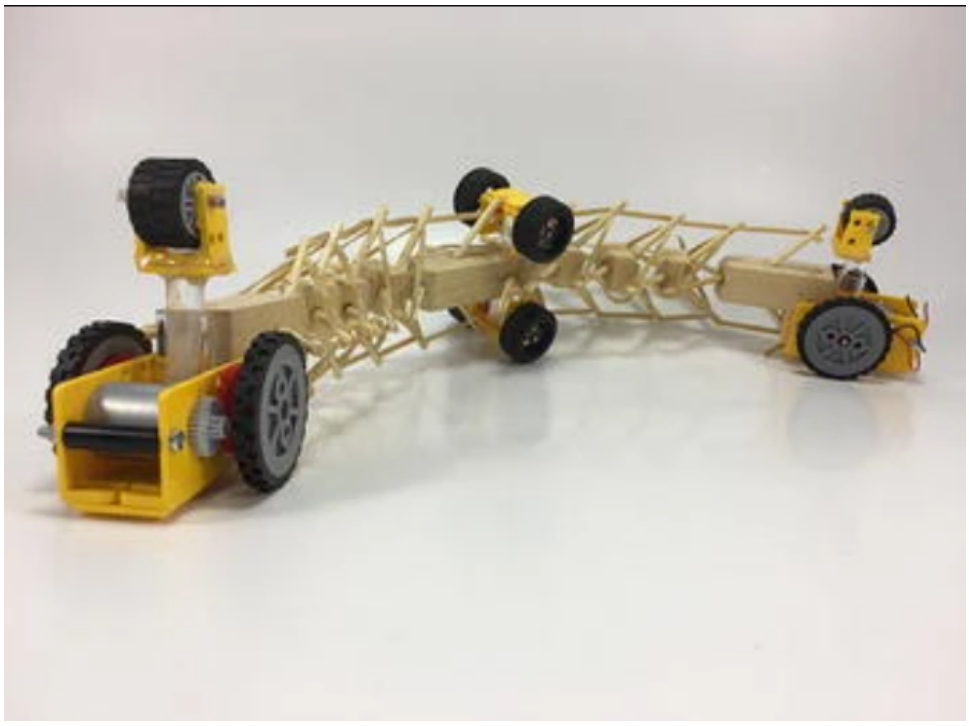

Figure 24: Wheeled tensegrity robot (WTR, taken from [6]) (It comprises three rigid structure.)

3 Design Principles

This chapter introduces a design of a tensegrity robotic snake, including its design objectives, force analysis and motion pattern analysis.

3.1 Design Objective

As described in the previous chapter, the design objectives of the robot snake for this project are as follows:

1. Adopt the tensegrity structure at the joint to make the robot have the characteristics of anti-impact and easy extension.
2. Make the structure able to mimic the way snakes move.
3. Make the design feasible. A physical prototype can be made for basic movement experiments.

Based on the above principles, the design idea of this project is to simplify the mechanical structure of the traditional tensegrity robotic snake (”Tetraspine”, as shown in Fig.22). Simplifying the tension structure can help reduce the installation of mechanical parts and electronic components, leaving more free space for the robotic snake to expand. This simplification is divided into two main levels. The first level is to introduce ground constraints on the mechanical structure. In this way, the emphasis of the tensegrity structure can be placed on the movement of the two-dimensional layer, which will change the tension network from three-dimensional to two-dimensional and reduce the complexity of the tension network. And the second level is about the simplification of control elements in tension network. In the tension network, the snake-like

robot can drive some motors to change the rope tension enough to create action. The other parts mainly provide tension structure stability, which can be replaced by springs to reduce the number of the motors that the overall need to install, freeing up more space.

According to the above ideas, this paper proposes the following design, as shown in the Fig.25. The basic motion patterns of the robot can be demonstrated with two identical modules, while a complete snake robot is scaleable and will link many modules in a chain.

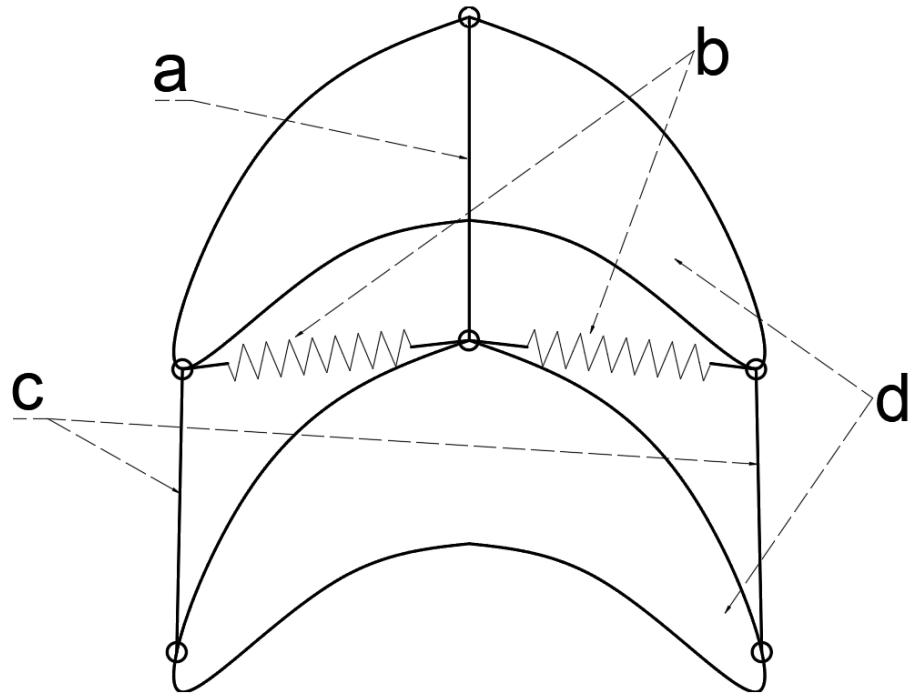

(a) Top view

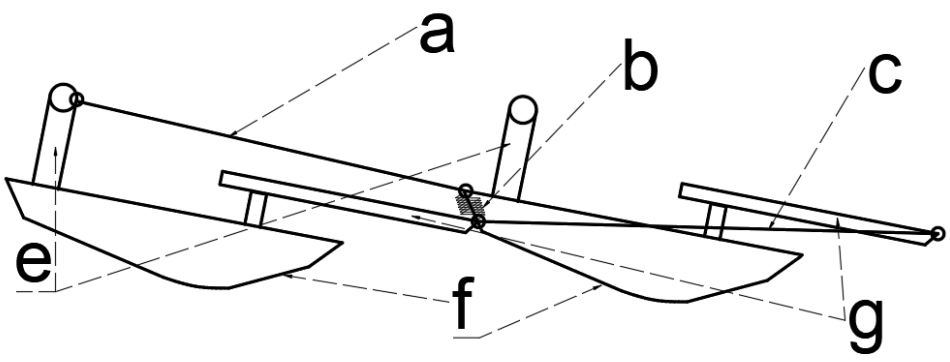

(b) Side view

Figure 25: Module construction.(a - distance control cable, b - spring, c - rotation control cables, d - main module body, e - hanging pulley, f - friction surface, g - rear wing)

This design consists of three drawstrings and two springs at each joint to form a tension network. And the bottom surface of each part is designed as two inclined surfaces with different friction coefficients. The effect of this design on the lower surface

is discussed in section 5.1 below.

To prevent ambiguity, some terms are specified here.

1. Each ”segment” or ”module” below refers to the independent rigid part connected by tension structures in the prototype, which is composed of the base, rear wing and electronic components on it.

2. Each ”flip” below refers to the tilting of the segment due to the change of tension structure, which makes the segment switch the surface touching the ground between the front lower surface and the rear lower surface. It is an intermediate stage between the pull and push stages of the segment.

3. Each ”rotate” below refers to the angle change of the segment around the normal direction of the ground.

3.2 Force Analysis of Structure

As shown in Fig.26, each pair of modules achieve rigidity through the tension of two springs and relative movement through the actuation of three cables. Each segment of the prototype has three motors, one is in the front of the body, and the other two are in the middle of the body, keeping the center of gravity of the joint easy to swing. They separately apply forces $f1$, $fl3$, $fr3$ through the pulley. Motion is divided into relative rotation between modules and linear distance change between modules, allowing combined serpentine and caterpillar motion.

Relative rotation of the module depends on cable forces $fl3$ and $fr3$. During straight movement, actuated cables will maintain tension, keeping the angle of the two modules

unchanged. To turn or achieve serpentine motion with many modules, one cable is tensioned while the other is loosened by motor control, causing the relative module angle to change while maintaining body equilibrium through spring forces $fl2$ and $fr2$.

Linear distance between modules is changed in two ways: through cable force $f1$ by equal change of cable forces $fl3$ and $fr3$, while spring forces $fl2$ and $fr2$ maintain rigidity of the structure. Forward caterpillar motion is facilitated by force $f1$ in two "push-pull" stages. In the "pull" stage, $f1$ is nearly zero, and the two modules are separated due to spring forces. The cable is then tensioned along $f1$ in the leading module, tilting the leading module upward and the trailing module downward due to $f1$ being above the center of mass, then pulling the modules together. The force $f1$ will increase the rear ground pressure of the first module and reduce that of the second module. As the module undersides are angled, this makes the friction of the leading module larger than that of the trailing module, dragging the trailing module forward. In the "push" stage, the cable at $f1$ is loosened, allowing $fl2$ and $fr2$ to tilt the modules parallel to the ground and decreasing the friction of the leading module, pushing it forward [18].

This is similar to the way western pythons move (as shown in Fig.27). The linear progression pattern of western pythons is fundamentally similar to that of some worms. During movement, they rely on the contraction and relaxation of the muscles to change the center of gravity of each part of the body, so that the body is stationary relative to the ground, to pull the rear parts that the muscles are connected to, so as to push the whole body forward. During this process, the vertebral column and its rigid connections can be maintained at a constant speed [1]. The tension network in the prototype acts as the muscle structure of western pythons, changing the pressure on the ground of

each part.

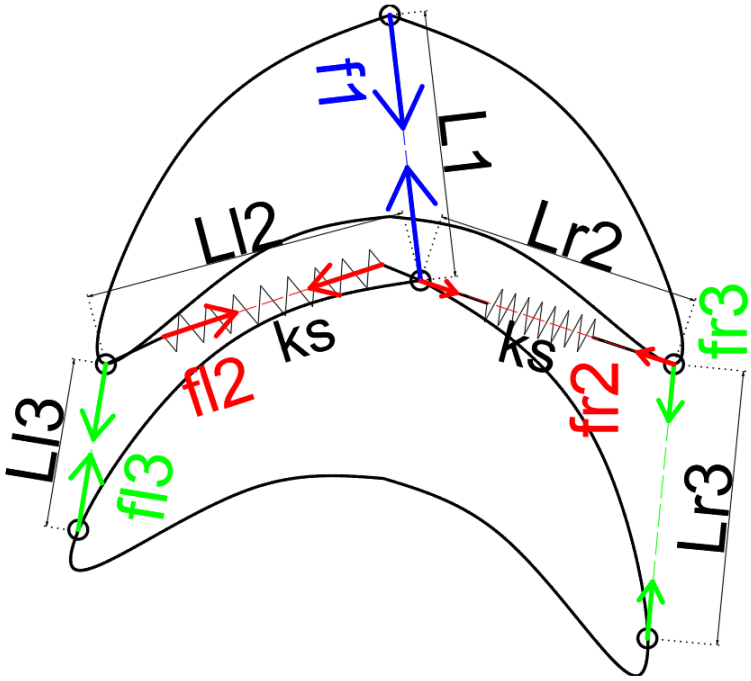

(a) Top view

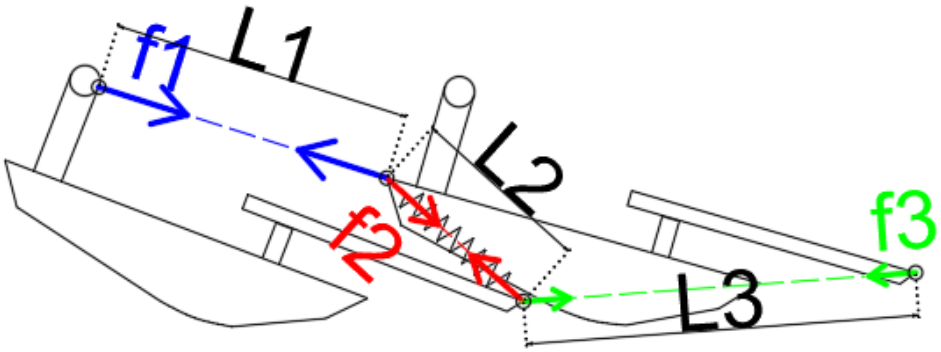

(b) Side view

Figure 26: Force analysis during module movement. (f1, f3 are the tensions applied to the corresponding tendons, L1,L3 are their lengths, L2 is the length of the spring, ks is the elastic coefficient of the spring, fl,Ll and fr, Lr indicate the left and right parts respectively)

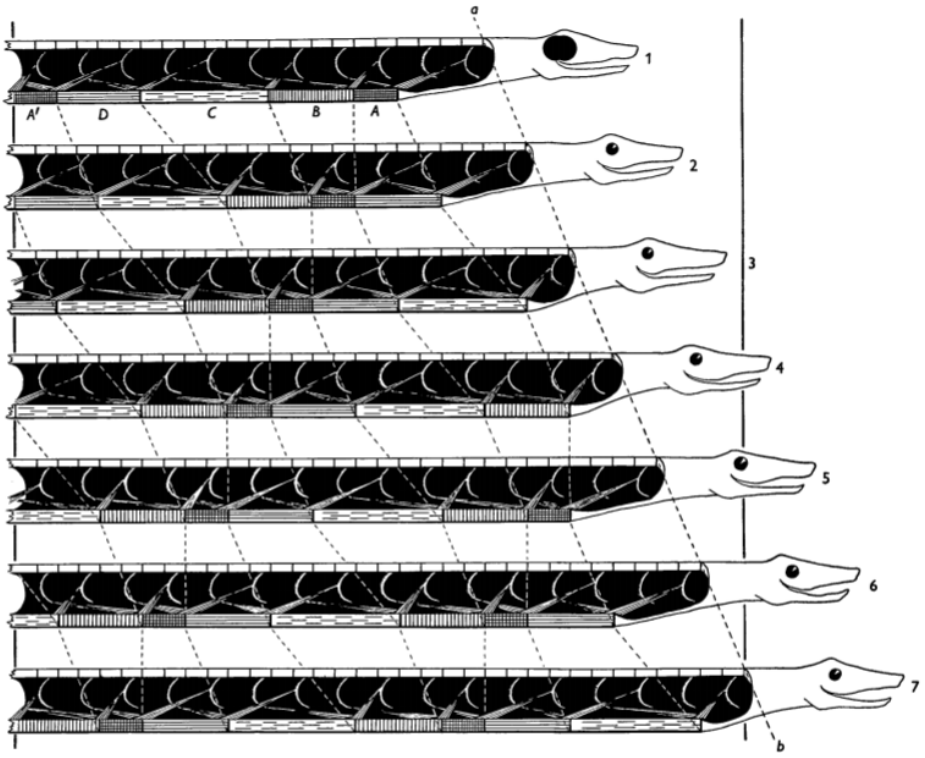

Figure 27: The way western pythons move

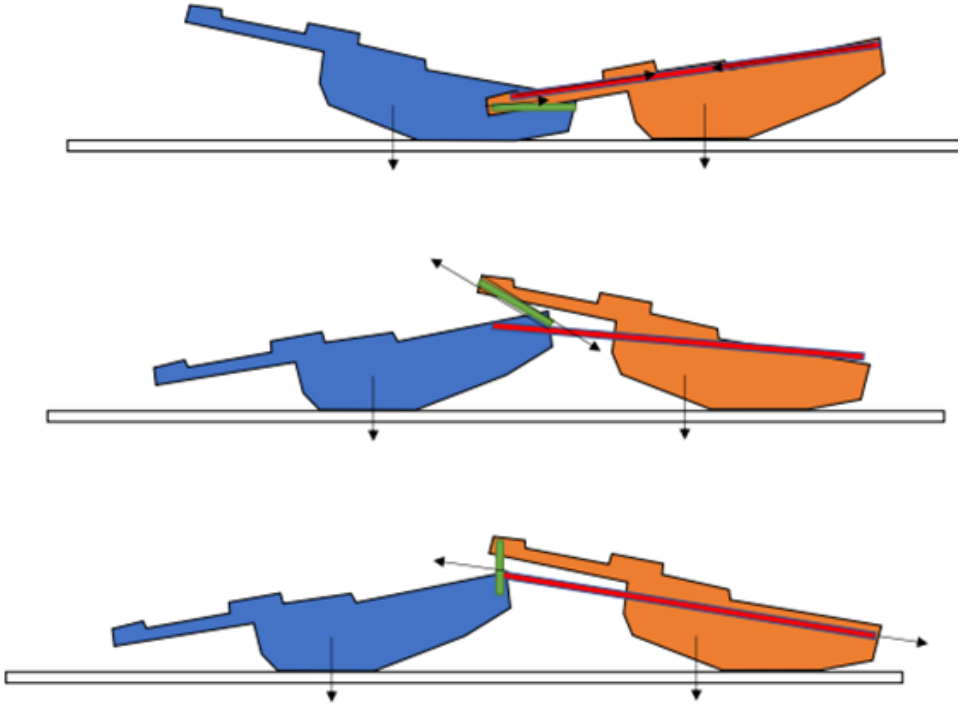

Figure 28: Schematic diagram of motion principle

3.3 Kinematic Movement of Prototype

Corresponding to force analysis, the linear motion scheme of the robot adopted in this design is caterpillar style, as shown in Fig.28. The core lies in making two parts push and pull each other through the tension network, and making use of the friction difference between the flipped parts in the process of pushing and pulling to make the two parts advance alternately.

Taking the two-segment prototype as an example, simplifying the force model during linear motion, the relationship between the force to the segments and the tension of the rope and the spring can be described with the formula 1 below. Assume that when the motor does not provide tension, the spring is the original length, which is also

tension-free.

$$F = F_1 - 2k \triangle l \cos\theta \tag{1}$$

In the equation, F is the force between the front segment and rear segment, F_1 is the main rope tension, k is the spring elasticity coefficient,$\triangle l$ is the length of elongation of the spring compared to that without tension (the left and right spring is symmetrical when the prototype is moving straight), θ is the angle between the spring and the advance direction of the prototype.

The ideal force situation is shown in the Fig.29, the main rope tension and spring tension alternating dominate the force between the segments, allowing each segment to move forward alternately. When the force is alternating, the segment will not move immediately (transition period for flipping), but will be flipped over first due to the change of the force direction, resulting the change the friction between the each segment and the ground (The change of tension makes the pressure on the ground of the segment change, and the friction coefficient of the segment touching the ground changes due to different surface materials.).

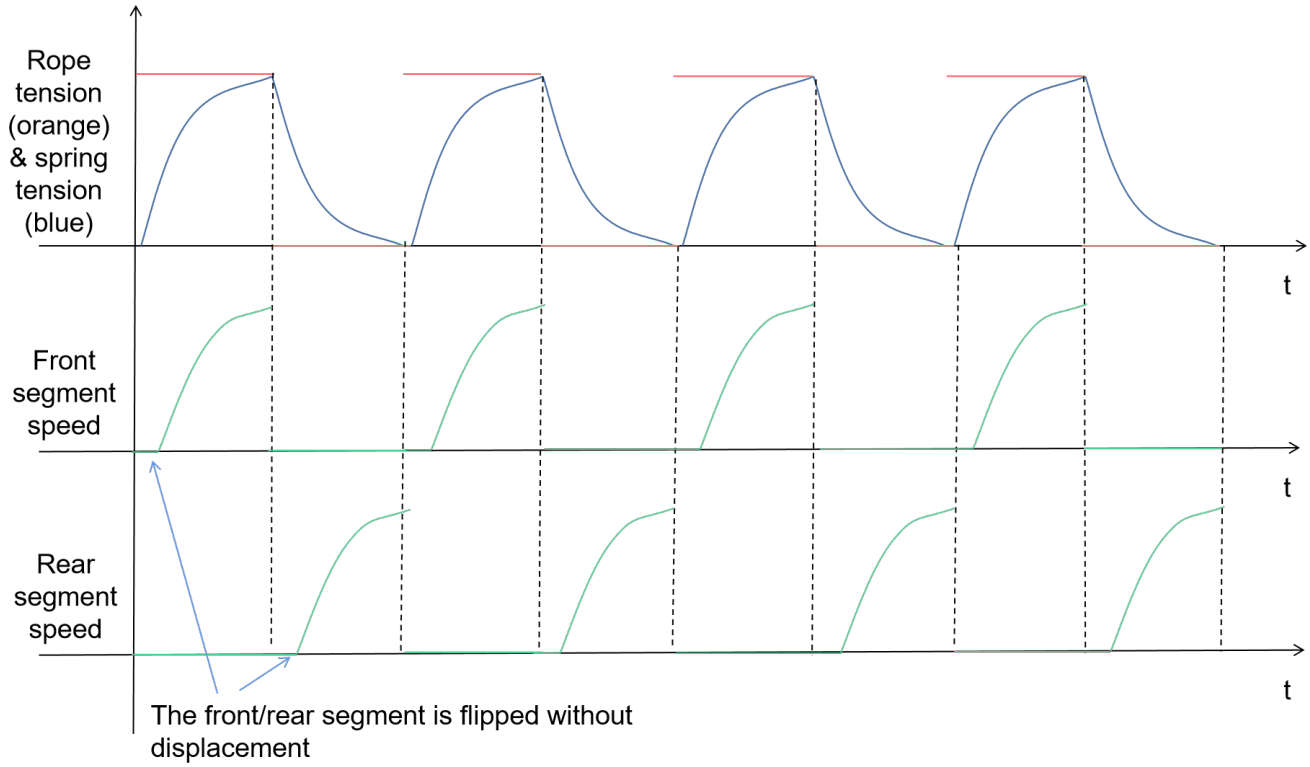

Figure 29: Ideal movement process of two-segment prototype

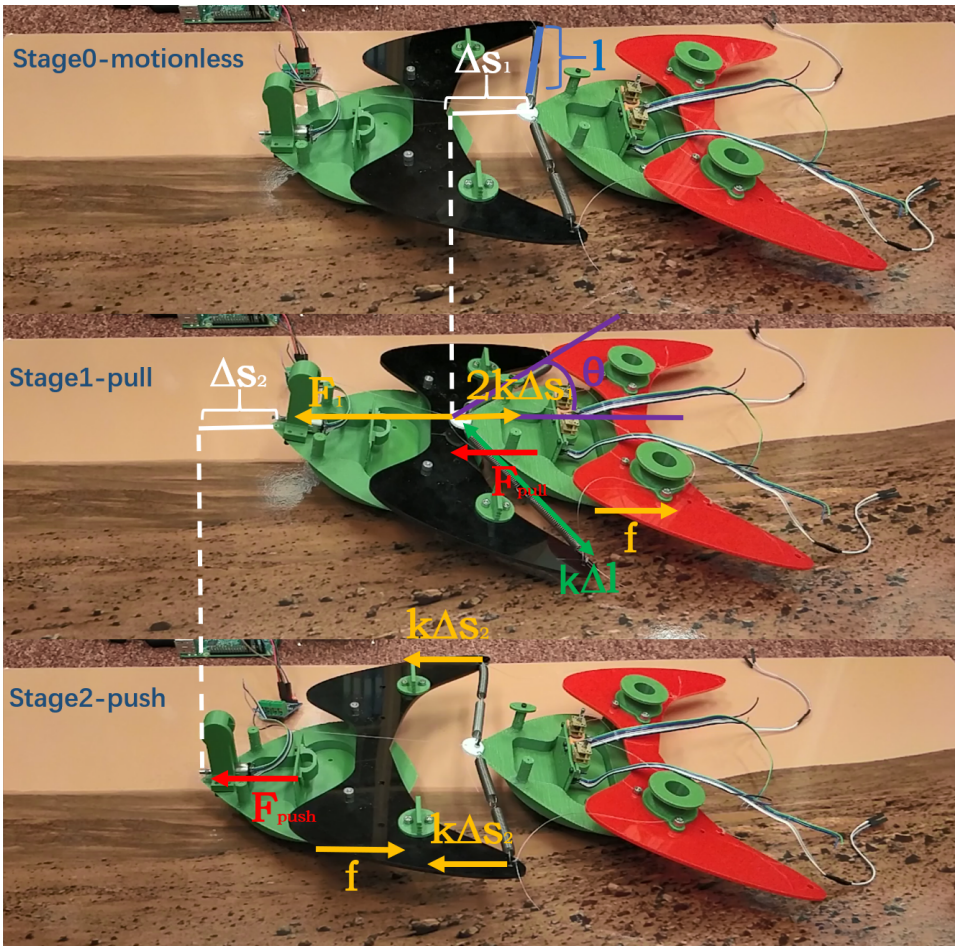

Figure 30: Schematic diagram of some symbols in the equation

The two-segment prototype is still taken as the ideal plane motion model. In the pull stage, equation 2,3,4,5,6 can be obtained. $\triangle s_1$ is the moving distance of the mobile module in the pull stage, $\triangle l$ is the change in length of the spring compared to the original length, θ is the angle between the spring and the forward direction of the module (acute Angle), F_{pull} is the resultant force on the mobile module of the prototype in the pull stage, C_1 represents a fixed constant, depending on the tension (F_1) and the ground friction of the mobile module (f), k is the elastic coefficient of spring, T_1 is the time of the pull phase, $v_{prototype}$ is the speed of the mobile module, $a_{prototype}$ is the acceleration of the mobile module, m represents the quality of the mobile module, t_1

represents the time from the start of the pull phase to the present. The Fig.30 shows some of the symbols in the equations.

$$\triangle s_1 = \triangle l \cos\theta \tag{2}$$

$$F_{pull} = C_1 - 2k \triangle s_1 \tag{3}$$

$$C_1 = F_1 - f \tag{4}$$

$$\triangle s_1 = \int_0^{T_1} v \mathrm{d}t = \int_0^{T_1} \mathrm{d}t_1 \int_0^{T_1} \frac{C_1 - 2k \triangle s_1}{m} \mathrm{d}t_1 \tag{5}$$

$$\triangle s_1 = -\frac{C_1}{2k} \cos(\sqrt{\frac{2k}{m}} t_1) + \frac{C_1}{2k} (\sqrt{\frac{2k}{m}} t_1 \in [0, \pi]) \tag{6}$$

(Detailed derivation is in the appendix.)

Similarly, s_2,C_1,F_{push},T_2,t_2 correspond to the physical quantities in the push stage. The similar equation 7,8,9 of the push stage can be derived. A more detailed derivation of the equation 6 and 9 can be found in the appendix. It is easy to find that the accumulated energy of the spring replaces the external force $F1$ given by the motor in the pull stage. In essence, the force curves change at the same rate with respect to distance in the pull and push stages. Only the initial force is different, so the distance traveled is expressed similarly in the equation.

$$F_{push} = C_2 - 2k \triangle s_2 \tag{7}$$

$$C_2 = 2kS_{1max} - f \tag{8}$$

$$\triangle s_2 = -\frac{C_2}{2k}\cos(\sqrt{\frac{2k}{m}}t_2) + \frac{C_2}{2k}(\sqrt{\frac{2k}{m}}t_2 \in [0,\pi]) \tag{9}$$

(Detailed derivation is in the appendix.)

Based on the above equation, it can be deduced that the moving speed of the two-segment prototype conforms to the equation 10,11. Thus, the relationship of force, time, moving distance and prototype speed in the pull stage is shown in the Fig.31. In the figure, C_1, k, and m are valued at 1. As a result, optimum T_1 is between 1.5 and 2, making the speed fast. It is also necessary to find out such a suitable time by testing the prototype in the subsequent experiments. T0 represents the time consumed by the transition stage between pull and push stages. To speed the robot up, T0 should be as small as possible, which means that the flip of the module should be done synchronously during the pull and push stage.

$$\overline{v_1} = \frac{S_1}{T_1} = \frac{\frac{C_1}{2k}(1-\cos\sqrt{\frac{2k}{m}}T_1)}{T_1} \tag{10}$$

$$\overline{v_{prototype}} = \frac{S_1+S_2}{T_1+T_2} = \frac{-\frac{C_1}{2k}\cos\sqrt{\frac{2k}{m}}T_1 + \frac{C_1+C_2}{2k} - \frac{C_2}{2k}\cos\sqrt{\frac{2k}{m}}T_2}{T_1+T_2} \tag{11}$$

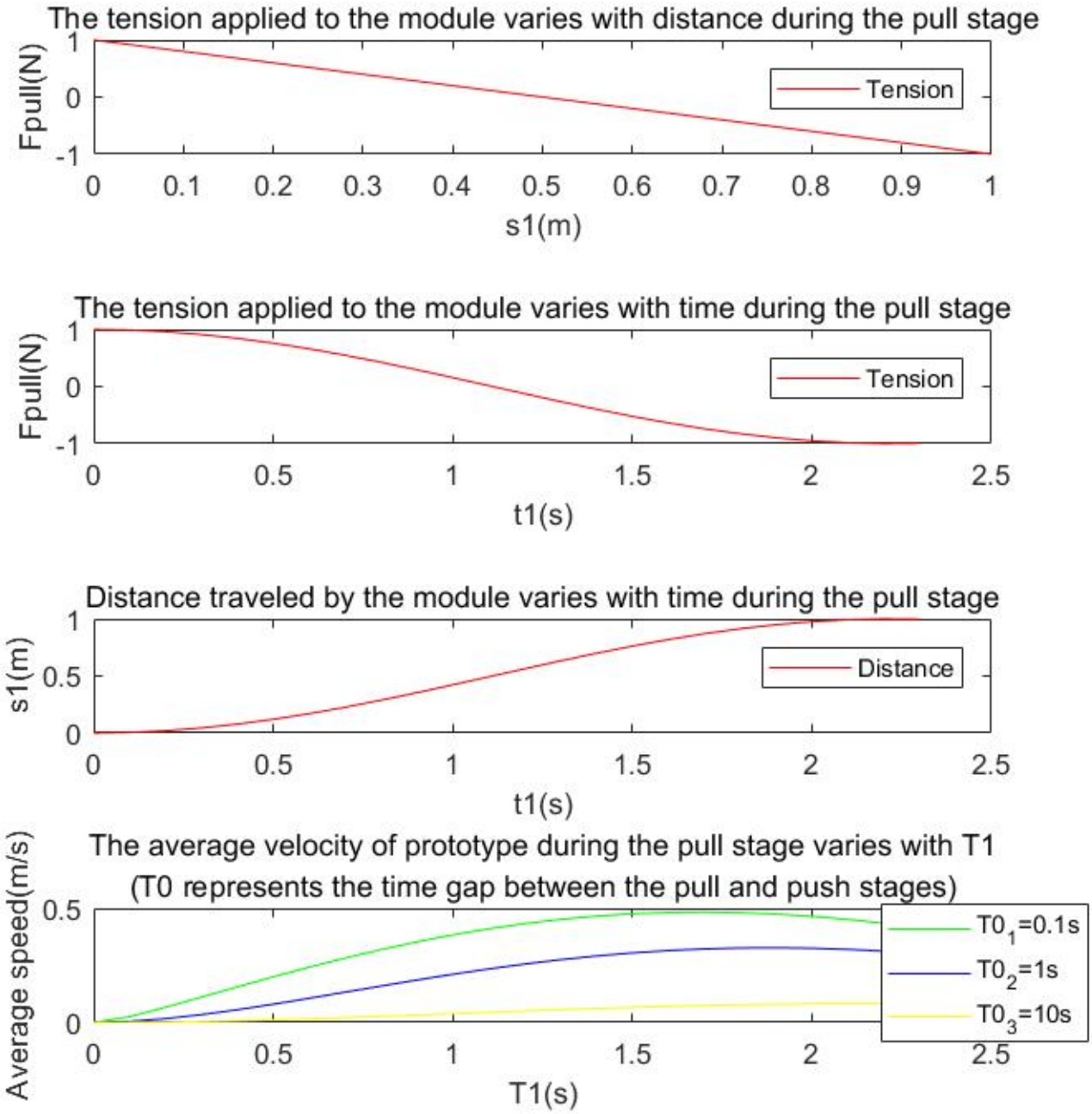

Figure 31: The relationship of force, time, moving distance and prototype speed in the pull stage

It can be seen from the velocity equation that the rising of tension C_1 (the rising tension F or the falling friction f) can improve the moving speed of the prototype. The increase of spring elasticity coefficient K, on the one hand, will improve the movement frequency, leading to smaller T_1 and T_2. On the other hand, it will shorten the moving distance, which is the step length of the prototype in the pull-push cycle. Therefore, the optimal speed can be obtained by balancing the step frequency and step length according to the spring elasticity coefficient, which is related to the ground friction force f and the tension force F_1.

The equation12 shows the relationship between C1 and C2. It's not hard to find that C1 is bigger than C2. This is mainly because the energy of the motor in the pull stage (T1) is consumed by friction and then converted into the spring energy released by the push stage (T2). The essence of C1 and C2 is the initial driving force on the module in the pull and push stage, so C2 will be smaller than C1. The suitable value (make the average speed the fastest) of T2 will also be faster than that of T1. As the number of modules increases, and many modules receive tension and thrust in the same period (as it flips forward), the values of T1 and T2 will converge.

$$C_2 = 2kS_{1max} - f = 2k * (-\frac{C_1}{2k}\cos\sqrt{\frac{2k}{m}}T_1 + \frac{C_1}{2k}) - f = (1 - \cos\sqrt{\frac{2k}{m}}T_1)C_1 - f \qquad (12)$$

The steering motion adopted in this scheme is based on linear motion. Known from the analysis of linear motion, in the process of linear motion, while one module moves, the other remains stationary. The part (flips backward) will be in static state. At this time, the motors on the left and right sides of the abdomen of the module can exert different tension ($f_l 3$ and $f_r 3$) on the tendons. And the module in the moving state (flips

forward), due to receive different tension on the left and right side, will rotate. Then when this module is stationary (flips backward), let the left and right tendon keep the same tension, so the rear module (flips forward) can follow the previous module to change direction.

3.4 The Expected Mode of Motion

On the basis of completing the basic movement of the module, the snake-like robot can try to perform the overall movement. Obviously, this motion pattern corresponds to the rectilinear movement of the snake.

Serpentine movement, which is the most common and balances energy consumption and forward efficiency, is that the snake can flip a longer part of the body to a certain extent to increase friction, and then move faster through muscle strength. Corresponding to the prototype, through the coordination of basic actions between modules, multiple modules can be slightly rolled to increase the friction so that faster movement of other parts of the body can be possible.

4 Detailed Prototype Design

Since the overall design of tension in this paper is involved in both rigid and flexible connections, it is difficult to build the ideal software simulation model as there is no robot simulation environment able to simulate both tensegrity dynamics and robotic control without significant development work, so this project focuses on evaluating a physical prototype. This chapter will elaborate on the design details of the prototype.

4.1 Hardware assembly of the Prototype

The components of the prototype can be classified into mechanical parts and electronic parts. The mechanical parts are the main body of the 3D printed modules and the tension structure composed of the motors, springs and fishing lines, and the electronic parts are the battery, Boost Converter Power Supply Module, STM32 ARM Development Board, and Bluetooth transceiver.

4.1.1 Mechanical Components

The main body of the modules is obtained through 3D printing, and the material is ABS. The rear wing of the prototype is a laser-cut acrylic plate. Mechanical components are shown in the Fig.32. The components and functions of each part are as follows.

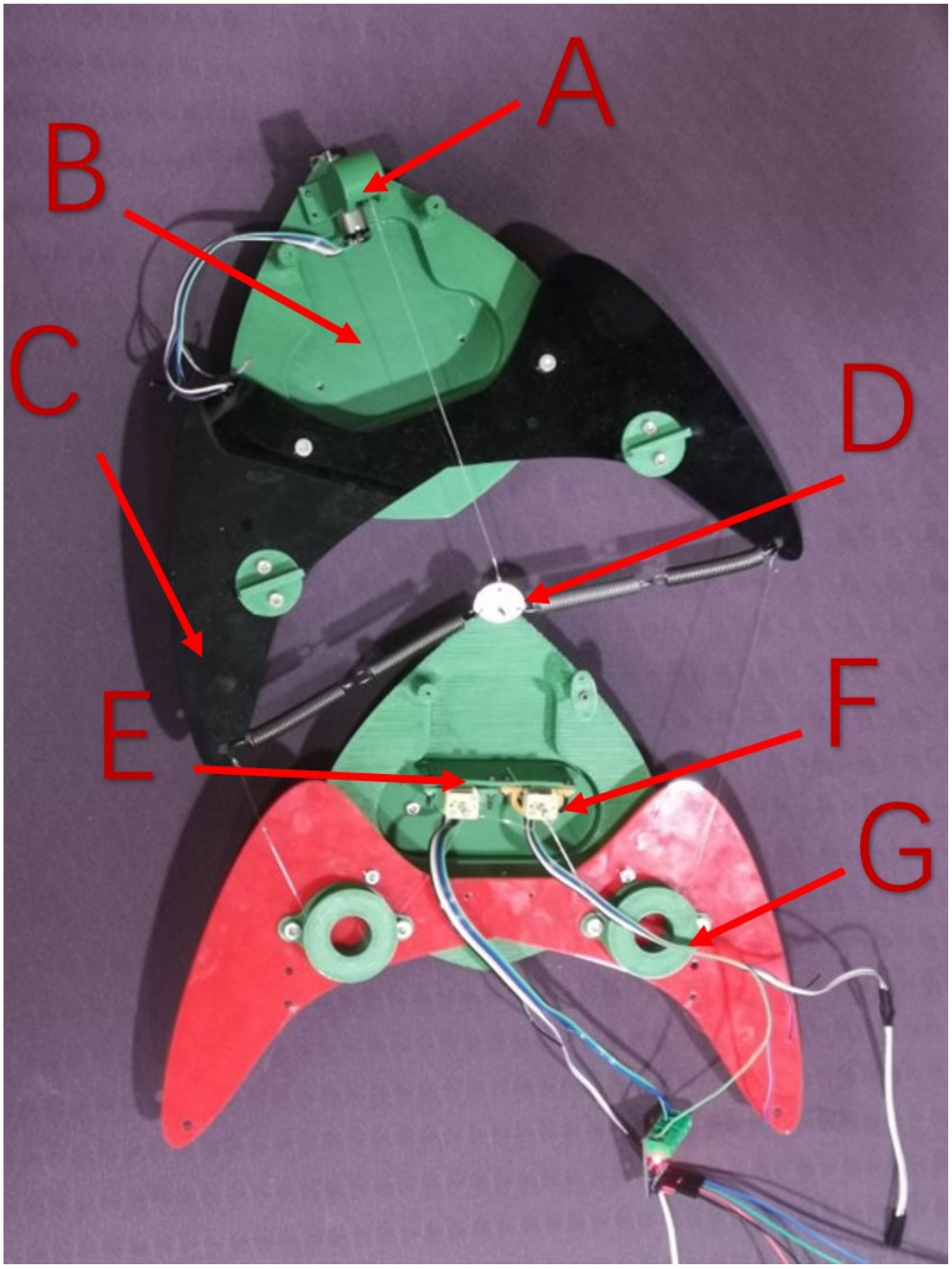

Figure 32: Schematic diagram of complete mechanical part

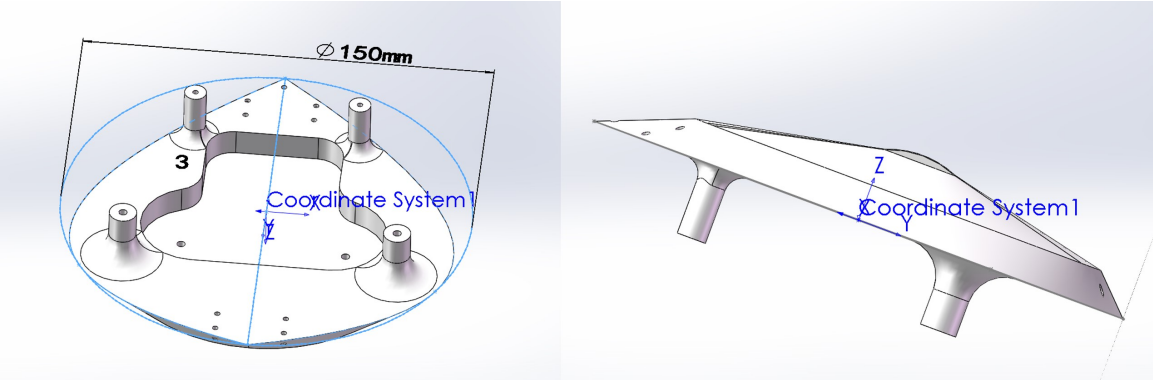

Figure 33: Base of module (B)

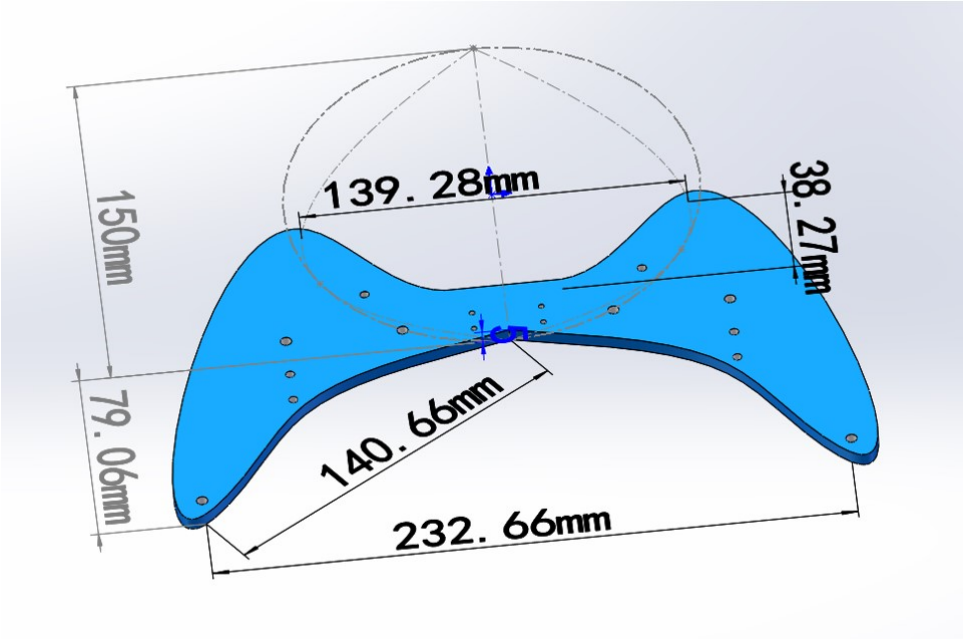

Figure 34: The rear wing of the module (C)

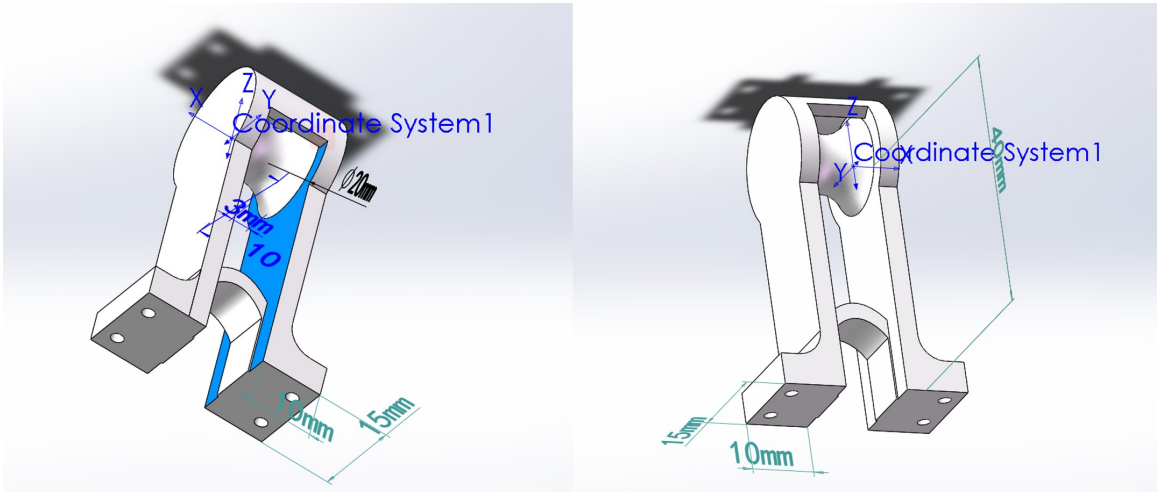

Figure 35: Main line pulley module (A)

As a whole, the prototype is constructed in this way. First, a large base is 3D printed, so that the lower surface can be flipped to touch the ground, while the upper part is reserved for installation (as shown in Fig.33). Then, laser cutting acrylic board was used to act as the rear wing of the prototype module (as shown in Fig.34), whose upper space was also reserved for installation, and then assembled to the bottom of the seat. Next is the motor mounting seat, which is mainly divided into the mounting seat of the main line motor (which is integrated with the pulley of the main line, as shown in Fig.35) and the mounting seat of the left and right line motor (as shown in Fig.36). After fixing the mounting seat and the motor, the pulleys (as shown in Fig.37) corresponding to the left and right fishing lines shall be installed. In this way, the main body of the mechanical part of the prototype module is completed. Finally, different modules are connected by fishing line and spring (as shown in Fig.38) to form the final prototype. The mechanical components has some special designs that need to be explained in detail.

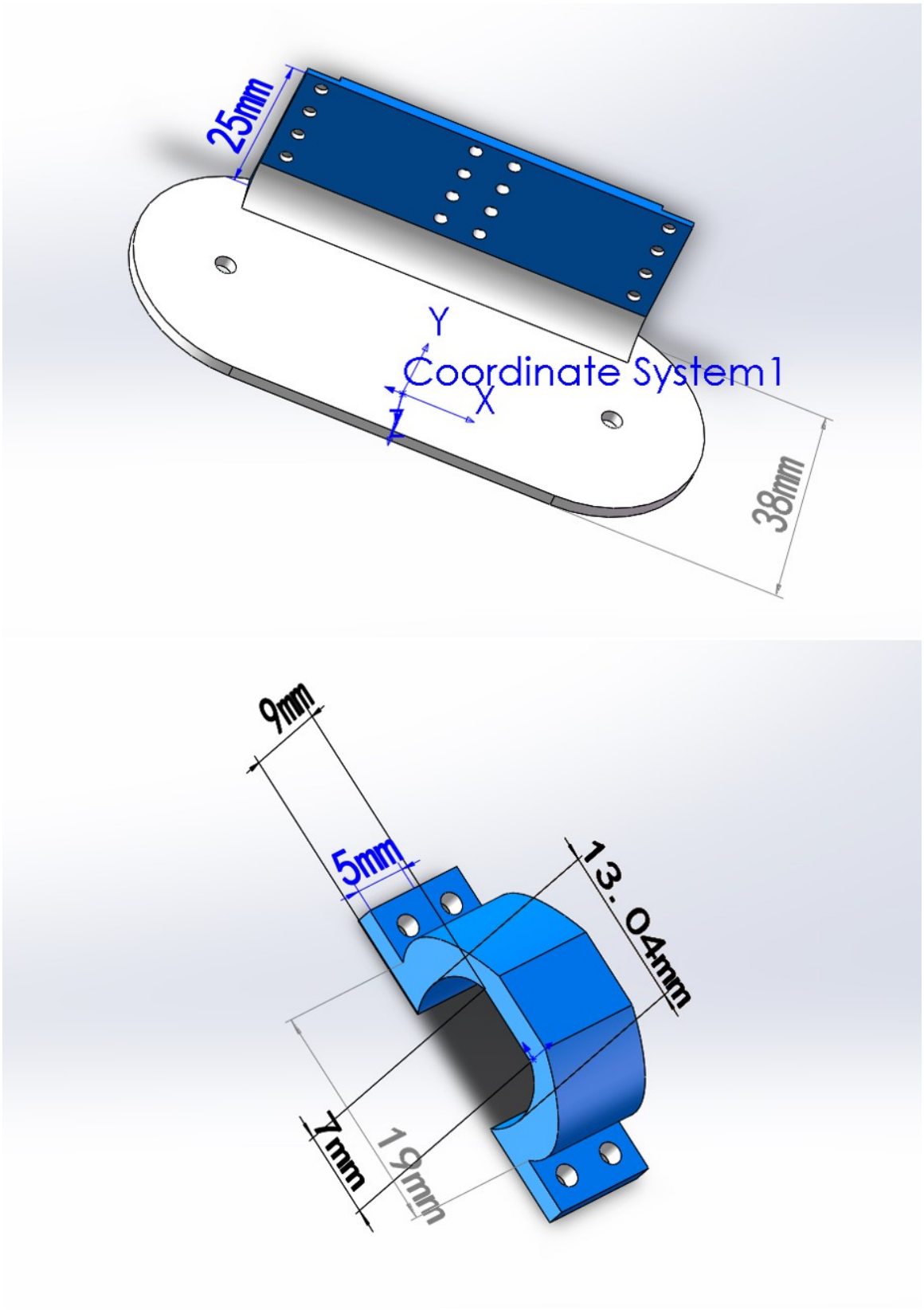

Figure 36: Motor mounting plate (E and F)

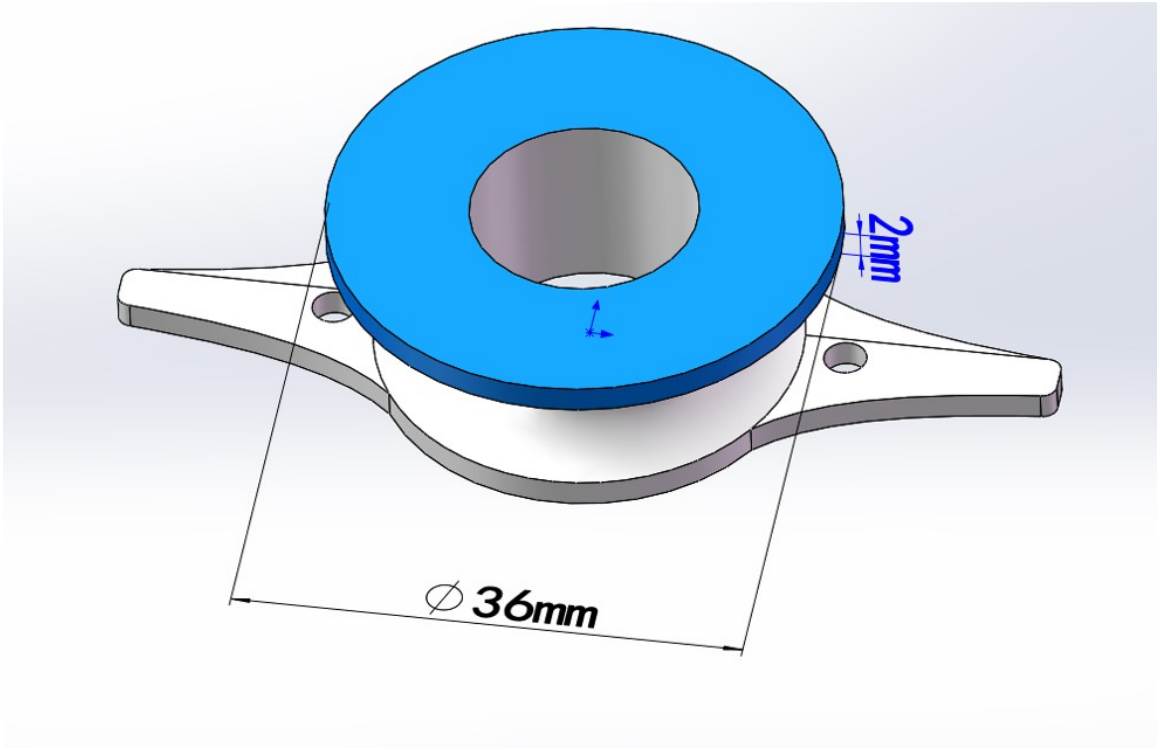

Figure 37: Left-right fishing line pulley module (G)

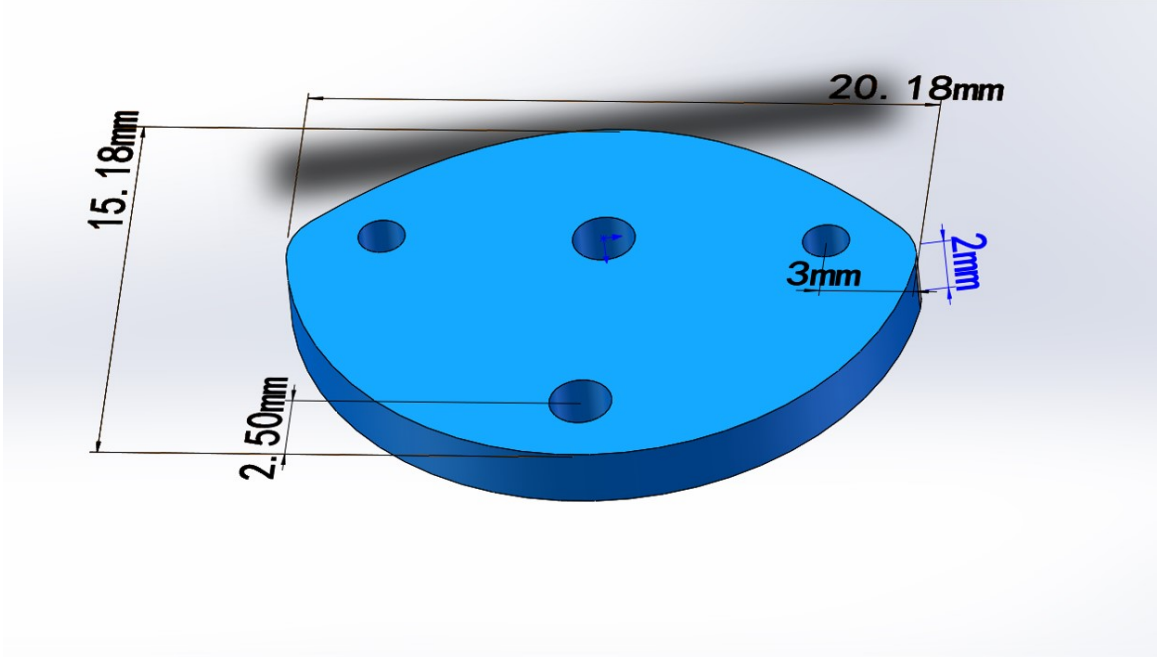

Figure 38: Connection link (D)

The most special aspect of the component B is its shape. Its lower surface consists

of two planes and a curved surface. Such a design is mainly for the convenience of the module in the pull and push stage to complete the flip movement. The front lower surface corresponds to the moving state, and the rear lower surface corresponds to the static state, the curved surface represents the transition of the stages. The shape on the horizontal plane of the component B is similar to water droplets, which is mainly to match the component C. The head of the component B and the tail of the component C are complementary, so that the prototype has enough free space to carry out movement.

Mechanical component A has a pulley designed to guide the fishing line wound on the motor. In addition to regulating the fishing line and avoiding the entanglement of the fishing line with other components, the main function of the pulley is to change the direction of the torque, so that the tension of the fishing line is applied to the pulley, thereby changing the pressure difference between the front and rear modules against the ground. In the pull stage, the fishing line exerted upward tension on the rear module to relieve the ground pressure of the rear module, while increased the pressure on the front module. Meanwhile, the pulley is subjected to downward force, while the motor installed in the front module is subjected to upward pull, which naturally drives the front module to flip. The front module flips backwards, and the springs on the rear wing presses down on the front part of the rear module, causing the rear module to flip forward. In the push stage, losing the pull of the motor, each module will be affected by the opposite force, making the opposite movement. The front module flips forward, and the rear module flips backwards. The Fig.39 shows the process.

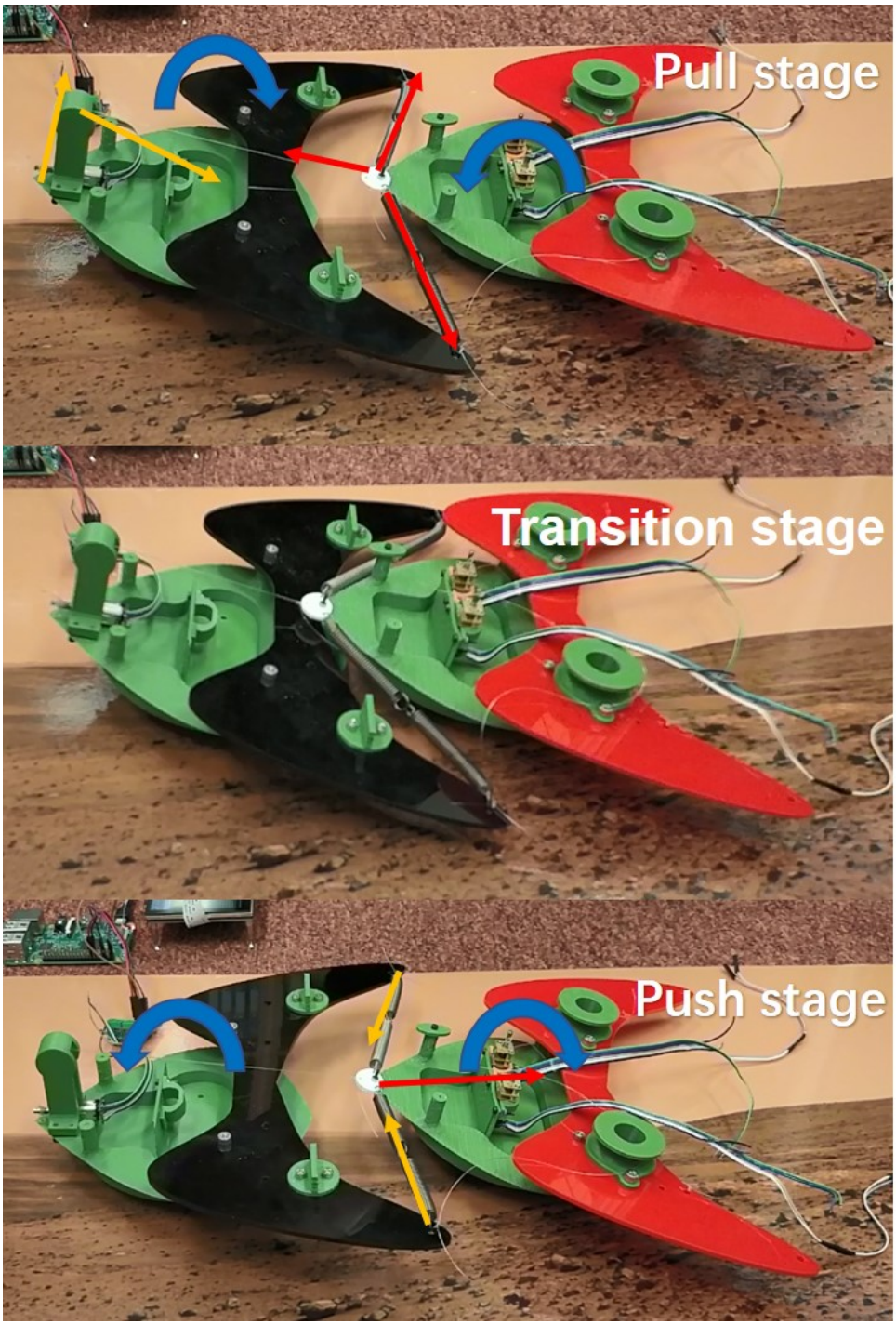

Figure 39: Schematic diagram of flip

This prototype was designed mainly to test the idea of motion, so a lot of details of the design were mainly based on empirical estimation, to keep it balanced in motion, and there was not a very strict quantitative study. In addition to the necessary mounting

holes in the components, there are some extra designs (such as extra mounting holes, extra parts), which were mainly used to test some other ideas in some experiment, but not much practical significance in this thesis.

Engineering documents for mechanical components can be obtained through the following link.

`https://drive.google.com/drive/folders/1vBYR5oibs0D4xF1Lx5bw-4yYGxL7Hu8f?usp=sharing`

4.1.2 Electronic Components

The electronic components of the prototype include STM32F103 main control core board, bluetooth module, voltage boost module, battery and motor drive board. The main function is to complete the control of the motor and the communication between modules. The complete electronic module relationship is shown in the Fig.40.

The pin resource allocation of STM32 chip is shown in the Tab.1. The system is mainly powered by the control panel (3.3V) and the motor (6V), which is realized by the battery and the booster module. The specific installation of electronic components is shown in the Fig.41. They are glued to the corresponding position by foam glue.

In order to control the motor to complete the control of tension network balance, the prototype needs to provide a drive module and a feedback module for the motor. In the meanwhile, the master control board also needs to be connected with bluetooth module to meet the needs of remotely controlling prototype.

It is worth noting that the bluetooth module is only used on the snakehead module (the first body module), and the coordination of multiple body modules is accomplished

through the wired USART communication between snakehead module and body module.

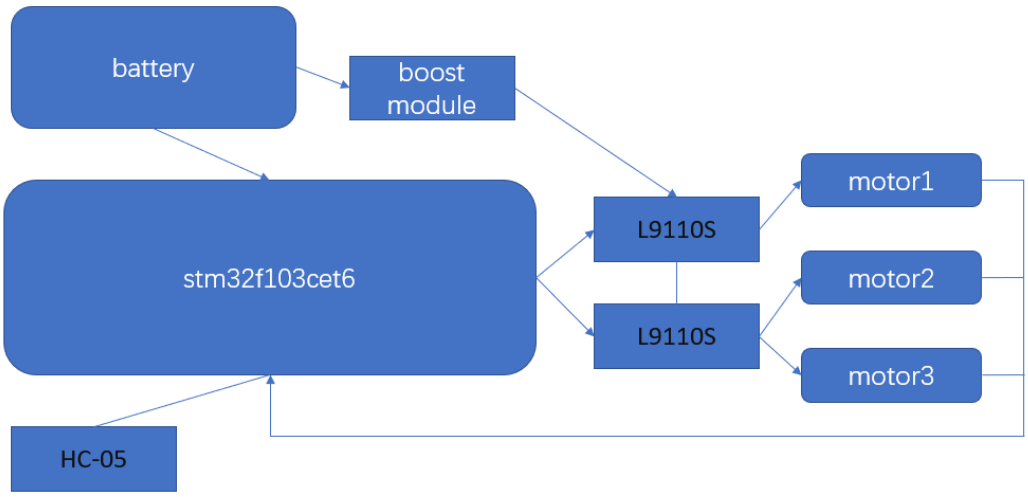

Figure 40: Schematic diagram of electronic module relationship

Table 1: Pin resource allocation for STM32 chip

	M1	M2	A	B
Motor (Main Line)	PA0-TIM2 CH1	PA1-TIM2 CH2	PA2-TIM2 CH3	PA3-TIM2 CH4
Motor (Left Line)	PA6-TIM3 CH1	PA7-TIM3 CH2	PB0-TIM4 CH1	PB1-TIM4 CH2
Motor (Right Line)	PB6-TIM3 CH3	PB7-TIM3 CH4	PB8-TIM4 CH3	PB9-TIM4 CH4
	Rxd	**Txd**		
Blueto oth	PB10-USAR T3_TX	PB11-USAR T3_RX		
Other stm32	PB10-USAR T1_TX	PB11-USAR T2_RX		

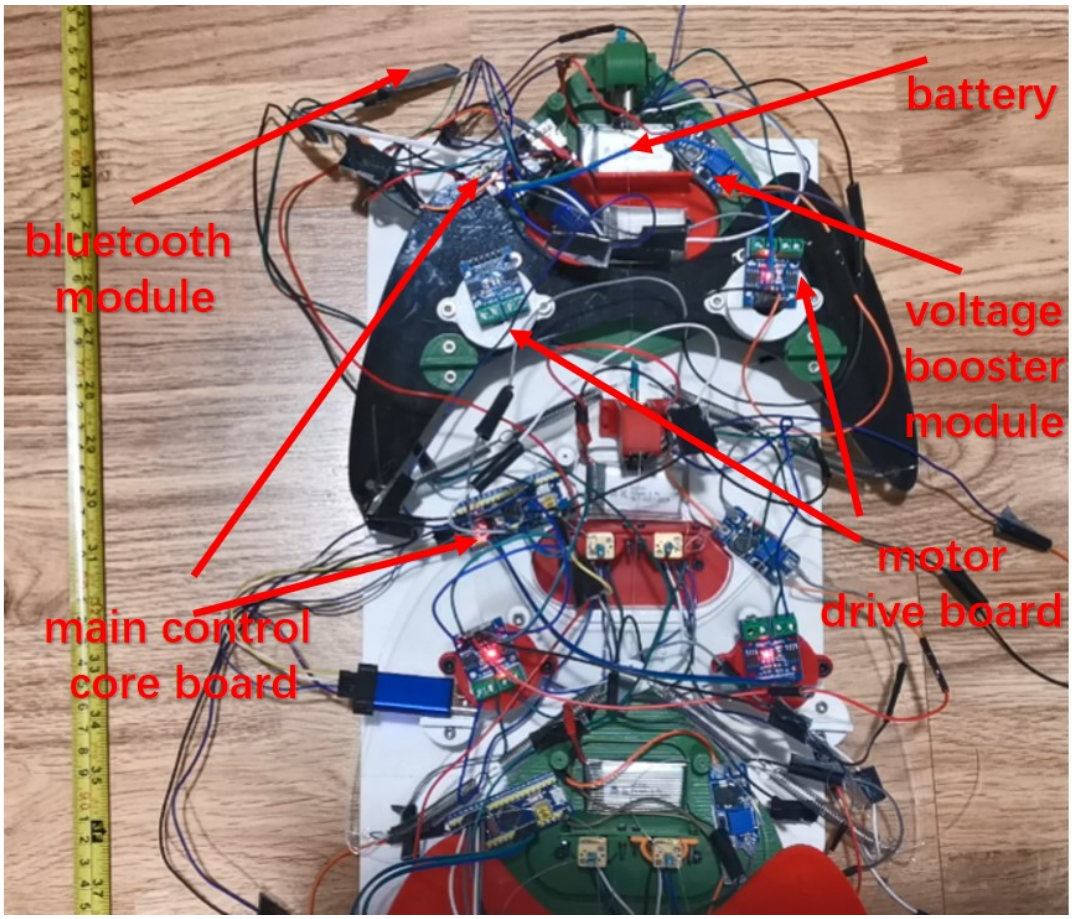

Figure 41: Schematic diagram of electronic components

4.2 Software Control of the Prototype

The software part of the prototype is mainly the control program written for the STM32F103 microcontroller. Relying on the FreeRTOS operating system, the software part completes the communication between modules, the switching of prototype motion modes and the motor control. The specific state mechanism is set up as shown in the Fig.42 below.

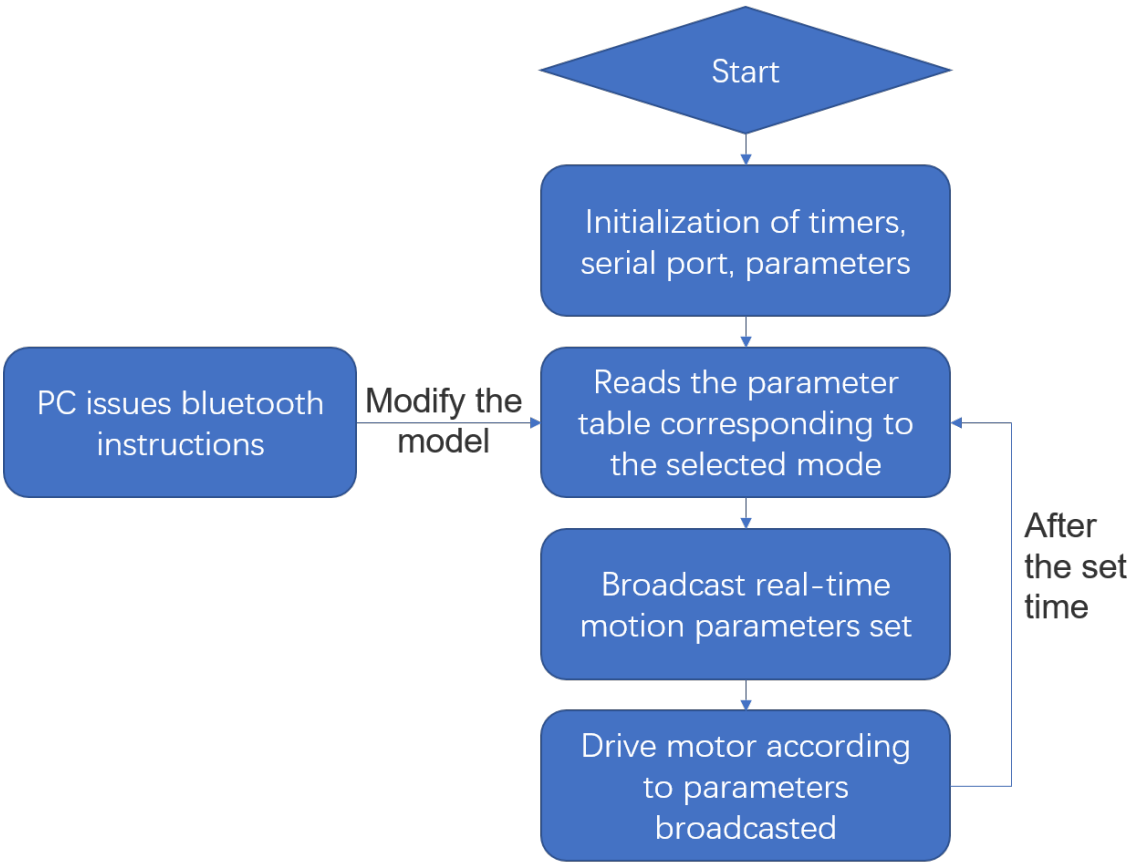

Figure 42: Program running process

4.2.1 Control System

FreeRTOS is a market-leading real-time operating system (RTOS) for microcontrollers and small microprocessors. Compared with other types of real-time operating systems, FreeRTOS has the following advantages:

1. FreeRTOS kernel supports preemption, cooperative and time slice scheduling.

2. It provides a Tickless mode for low power consumption.

3. FreeRTOS-mpu supports MPU units in the CoREx-M series, such as STM32F103.

4. FreeRTOS system is simple, small and easy to use. Usually, the kernel takes up

4K-9K bytes of space.

Through the FreeRTOS system, the software realizes the scheduling and switching of communication tasks, prototype states, switching tasks, and motor control tasks, to facilitate varied experiments with the prototype.

4.2.2 Communication between Modules

The communication to the prototype is accomplished through USART ports, mainly between a PC, snakehead module and body modules. The PC communicates with the snakehead module via Bluetooth, while the snakehead communicates with the body module via stranded wires. During the movement, the snakehead part receives instructions from the PC and broadcasts the planned motor movement parameters to the body modules.

4.2.3 Motion Mode Switch

Since the prototype is mainly used for testing, the ability to switch between different parameters is essential. There are two modes of motion. First, the bluetooth control mode. In this mode, the prototype follows commands from the PC to modify the motion parameters of motors in each body modules. This mode is very suitable for early motion planning for prototype. Because this type of structure is difficult to simulate, many details of prototype production are not carefully considered and calculated, so this mode is needed to adjust the motion of the prototype remotely. By observing the performance of the prototype with different motion parameters (such as the voltage duty cycle of the driving motor and time of each stages), a universal motion parameter

can be found.

The second mode is tabular parameter reading mode. This mode relies on the motor parameter table drawn up in the program and reads the table to modify the motor parameters according to the timer to realize the motion between modules. This mode is mainly used in the field test after the prototype parameters are determined.

4.2.4 Motor Control

In the design process, the original plan was to use the PID speed loop and position loop control motor, but given the core of tension network change lies in the change of tension, it is difficult to get a good effect with quantitative fine control without theoretical calculations because the speed and distance of the fishlines are not directly related to the tension, so in this generation of prototype, we use simple PWM duty cycle change to control the tension of the line, directly through the change of the tension to control the movement of this tensegrity structure.

4.2.5 Control Strategy

The motion control of wheeled and wheeled snake-like robots requires radically different approaches [4][25]. This design is to study robotic snakes without wheels, which perform basic movement tests with open loop control. The gait of the prototype, as described in the section 3.3, is achieved through the cycle of the pull and push stage. Due to the lack of simulation and theoretical guidance, the motion parameters of the prototype need to be obtained in the experiment. The tension exerted by the motor, the time to exert the tension and the time of the stages can be adjusted. By recording

its performance, the appropriate parameters can be obtained. In the case of ensuring that the motion is robust, speed will be the most important consideration.

In the later stage, the control strategy can be improved. There are many relevant cases to refer to. Considering the use of the friction on the surface, the snake-like robot could move better with the help of obstacles through design and planning [50]. In terms of obstacle avoidance, a force feedback system can also be built to help the robot understand the environment through force so as to overcome obstacles [16]. However, due to the limited time of this project, there is no further study on the control strategy about obstacles in this thesis.

5 Experiments and Results

The specific task of the original prototype is to explore the performance of the tensegrity structure on different terrains and the related factors that affect its movement, so as to make suggestions about the modification of the next generation of robotic snake. The smooth floor, ordinary paper surface, rough carpet, rough road surface, floor tile surfaces and ramps are selected as the experimental terrains. In addition to exploring the impact of structure and terrain on the rectilinear movement of the prototype, the experiments also tested the steering and serpentine motion of the prototype.

5.1 Lower Surface Covering

At the beginning of the experiments, the influence of the lower surface covering on the motion of the prototype was tested. In the process of rectilinear movement, the difference of the friction at the bottom of the module comes from the pressure difference caused by the change of the tensegrity structure on the one hand, and the different covering materials on the front and rear lower surfaces of the prototype on the other hand.

Experiments found that with the increase of battery mass and other components, the tension and thrust from the tensegrity structure is not enough to produce enough pressure difference between prototype modules, so in the process of travel, if the prototype didn't add a lower surface covering, it would appear to exhibit an obvious backward travel phenomenon, namely the various modules relative to the ground will move at the same time alternately close to each other and far away from each other, making the prototype unable to move forward effectively.

After adding different friction materials to the front and rear lower surfaces of the module (as shown in Fig.43). It was found that the friction against the ground of the static and dynamic modules during each movement could be significantly differentiated, thus the prototype could effectively move forward. In the experiments, the front lower surface was covered with adhesive tape, while the rear lower surface was covered with fragments of a yoga mat. Obviously, the surface of adhesive tape is very smooth, while the yoga mat fragments are rough, such addition reduces the friction when the module is moving (as it flips forward), and increases the friction when the module is stagnant (as it flips backward).

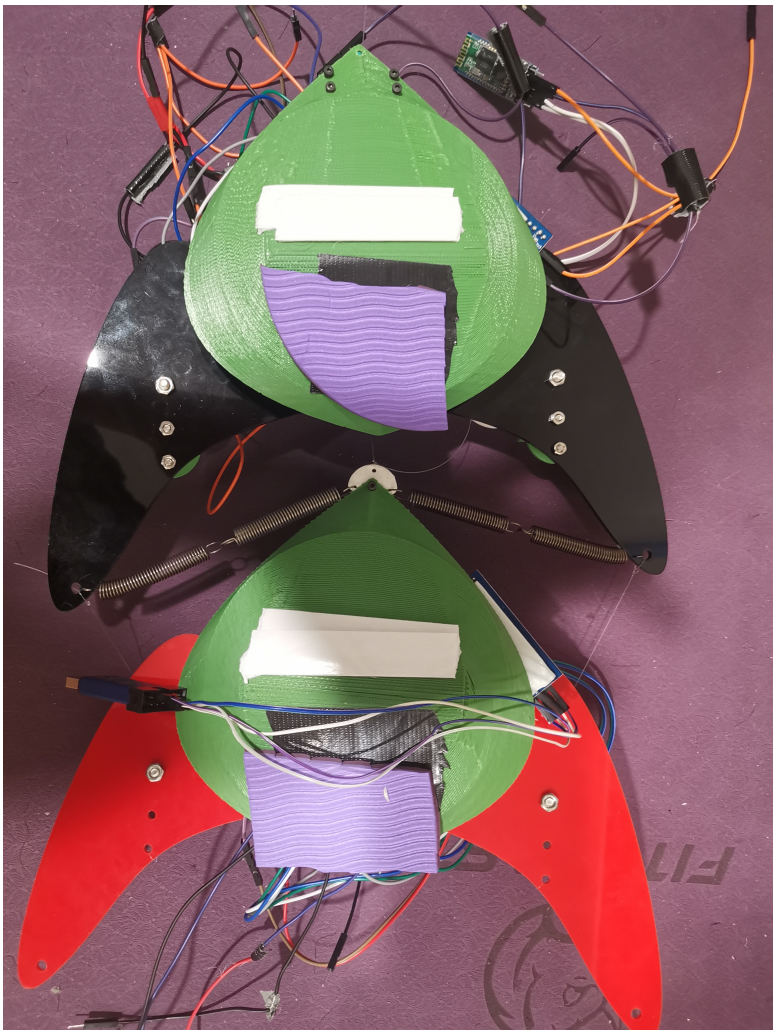

Figure 43: Different materials are used for the front and rear lower surfaces, the front lower surface was covered with adhesive tape, while the rear lower surface was covered with fragments of a yoga mat.

5.2 The Spring Elasticity Coefficient and The Corresponding Tension Change

The elastic coefficient of the spring and the corresponding tension change determine the motion rhythm of the module, which is manifested as the step length and switching

frequency of the pull stage and the push stage in the prototype movement.

Smooth floors (as shown in Fig.44) are ideal terrain for basic validation and analysis. The next experiment mainly tested the influence of the spring in the structure and the tension exerted by the motor on the overall speed. This part of the experiments was completed by a two-segment prototype, as shown in Fig.45.

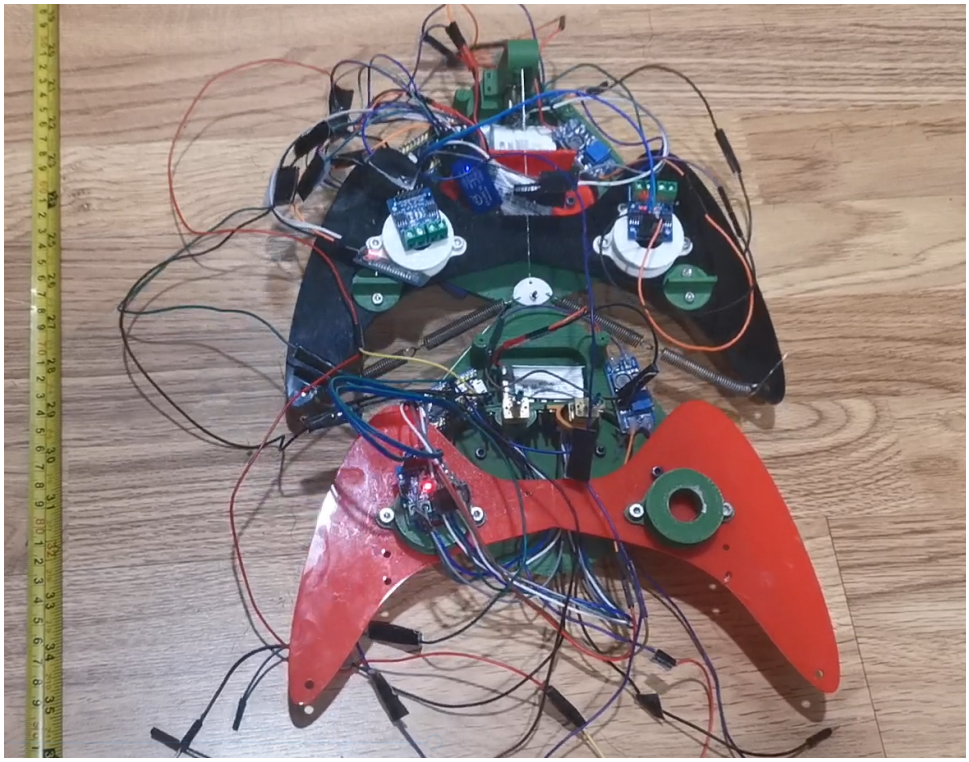

Figure 44: Schematic diagram of smooth floor

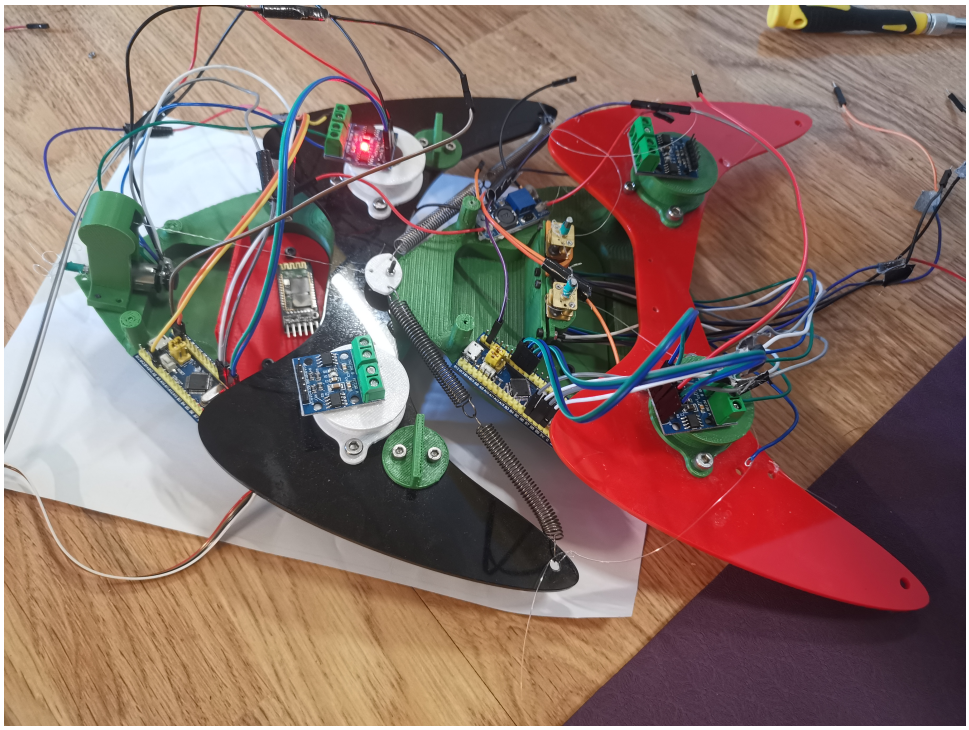

Figure 45: Schematic diagram of the two-segment prototype used in the experiment

Table 2: The linear motion results of the two-segment prototype with different spring coefficients and different motor pulling force

No.	the coefficient of spring	duty cycle of high level (PWM of the motor)	T1(s)	T2(s)	test area	the average moving step size (cm)	the average speed of prototype (cm/s)
1	small	1	0.8	0.5	floor	2.87	1.94
2	small	2/3	0.7	0.4	floor	1.59	1.42
3	big	1	0.8	0.5	floor	2	1.4

The results of the experiments are shown in the Tab.2. The yellow column in the table is the independent variable of the experiments, and the blue column is the dependent variable. The results of the experiment are discussed in detail below.

The main difference between Experiment 1 and Experiment 2 is the tension provided by the motor at the head of the module. The second experiment used a smaller pull, and the changes in T1 and T2 were adjusted to accommodate the smaller pull. In the experiment, the experimenter set several groups of T1 and T2 for comparison, and finally selected the value with the fastest moving speed. The reasons for this result are as follows:

Under the condition that runs at full power (Experiment 1 and 3), T1 was set to 0.8s, T2 was set to 0.5s. And if the tension of the motor was reduced (Experiment 2), T1 was changed into 0.7s, T2 was changed into 0.4s. This is because the tension decreases, and the period of actual motion is also reduced, so the higher the T1 and T2 and is not able to bring the speed improvements, as shown in Fig.31 in section 5. Excessive T1, T2 will make prototype to stay in the motion of the decelerating trend, which reduces the average speed.

The other thing needs to be explained is that T1 was set to be larger than T2. This is because in T1 it is the motor that drives the module to move, while in T2 it is the spring that drives the module to move. The energy of the spring comes from the storage of the motor tension in pull stage (T1), and the energy of the motor is converted into the stored energy of the spring after the consumption of the friction in the pull stage, so the module releases more energy at T1 than it does at T2, making the pull stage (T1) of the module is longer than the push stage (T2).

From the results of Experiment 1 and Experiment 3, it is obvious that the prototype moves faster when the tension is larger (without damaging the stability of the motion). This makes perfect sense, because in the case of T1, T2 being the same, the module

accelerates more with greater tension. Then adjusting T1 and T2 (to accommodate changes in the actual motion period) also allows for faster speeds.

The relationship between speed and step size is positively correlated. The longer the step length is, the higher the overall moving efficiency and speed of the prototype is, regardless of the coefficient of elasticity of the spring applied. This conforms to the analysis in section 3.3 – in order to achieve a large movement speed, each period should be close to the time position where the force between modules is nearly reset to zero (as shown in the Fig.30), which is also close to the limit of step size.

From the results of Experiment 1 and Experiment 3, the selection of springs with different elastic coefficients will also affect the efficiency of motion mode. A higher spring coefficient means that, if the same tensile force is applied, the module would travel less distance. However, due to the motion inertia of the module, the module cannot complete the turnover in a shorter time, so T1 and T2 cannot be reduced and the step frequency cannot be increased. In this case, the smaller the step distance leads to the smaller the speed.

However, if the prototype moves on the surface with a greater friction coefficient, the prototype with a larger spring can also adopt a larger step size. Therefore, a spring with a larger elasticity coefficient can help the prototype adapt to more rough terrain.

5.3 Influence of Surface Friction

In simple terms, smooth surfaces are more conducive to increasing the effective step size and thus the overall speed, compared with rough surfaces. Within the elastic limit of the spring, the friction coefficient of the ground and the size of the prototype

determine the maximum step. The smooth plane allows the prototype to move faster on the ground.

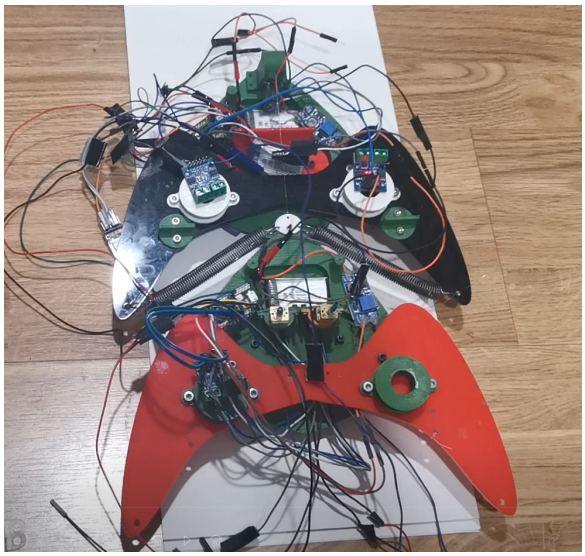

Figure 46: Ordinary paper surface

Figure 47: Rough carpet

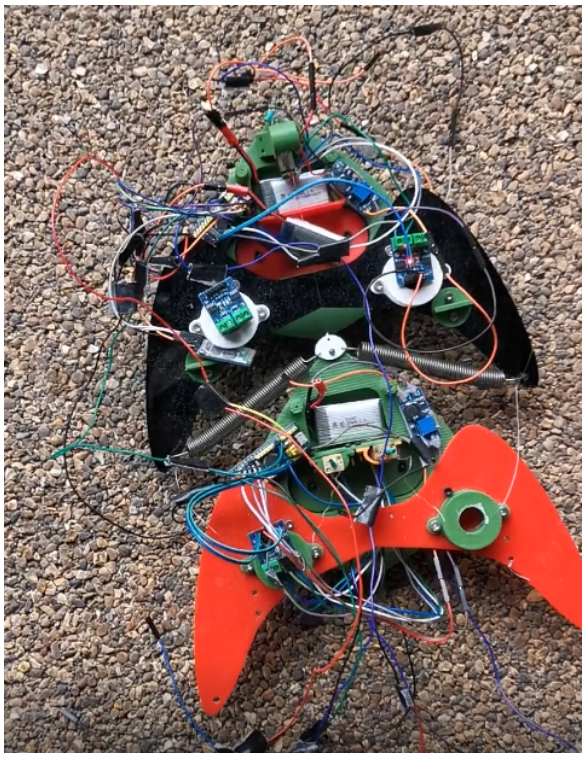

Figure 48: Rough road surface

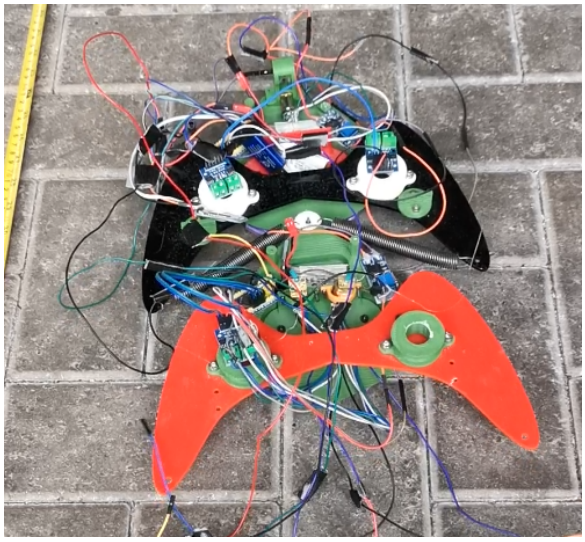

Figure 49: Floor tile

The experimental results on the smooth floor, ordinary paper surface (as shown in Fig.46), rough carpet (as shown in Fig.47), rough road surface (as shown in Fig.48),

floor tile (as shown in Fig.49) are shown in the Tab.3. In these experiments, the prototype used large springs and the same motion parameters, and it could be found that the linear advance of the prototype has better results on the floor and paper. On rough terrain, the overall speed is slow due to the decrease in step size.

Table 3: The linear motion results of the two-segment prototype on different surfaces

No.	the coefficient of spring	duty cycle of high level (PWM of the motor)	T1(s)	T2(s)	test area	the average speed of prototype (cm/s)	the average moving step size (cm)
4	big	1	0.8	0.5	floor	1.4	2
5	big	1	0.8	0.5	carpet	1.19	1.72
6	big	1	0.8	0.5	floor tile	1.21	1.87
7	big	1	0.8	0.5	coarse ground	1.35	1.93
8	big	1	0.8	0.5	paper	1.8	2.6

5.4 Climbing Experiment

The climbing experiments were carried out on two slopes (as shown in the Tab.4) with a slope of about 12°, one of which used a relatively rough paper surface as the surface climb and the other used the smooth plastic surface. The experimental results (as shown in the Fig.50) show that the roughness still have effect on the speed of the prototype.

Table 4: The linear motion results of the two-segment prototype on the slope

No.	the coefficient of spring	duty cycle of high level (PWM of the motor)	T1(s)	T2(s)	test area	the average speed of prototype (cm/s)	the average moving step size (cm)
9	big	1	0.8	0.5	slope (paper surface)	1.81	2.85
10	big	1	0.8	0.5	slope (plastic film surface)	0.8	1.3

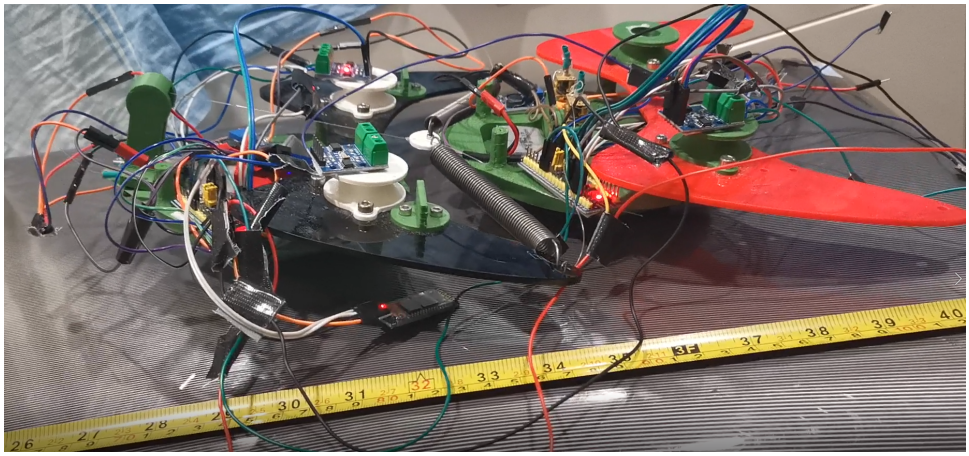

Figure 50: Advance on the slope

It is important to note that although Experiment 9 was on the paper slope, but did not differ a lot about the speed compared to the ground (Experiment 8). The component of gravity along the slope should decrease the step size of the prototype, but in the experiment, step size did not decrease. According to the analysis of experimental video, it is probably because the slope makes the prototype flip more quickly compared to the ground. In the previous cases, the flip of a module affects movement. Forces are used for flipping rather than movement over a period of time, namely T0. The prototype on the slope flips more quickly, which makes the time of effective movement

longer. Therefore, in the same control period (T1+T2), the actual T0 of the module on the slope is smaller than that on the ground, which makes the step length of the prototype on the slope not significantly less, and the overall speed was not affected much. Therefore, the distribution of the center of gravity of the module has an impact on the movement of the robotic snake in different planes, which needs further study. On the one hand, it reduces the push and pull on the module, but on the other hand, it reduces the transition time T0.

In addition, when the experiment was carried out on a slope of more than 15°. Once the prototype starts moving, it would slide straight down the slide. This is because the prototype has too few joints and the friction coefficient of the materials used on the lower surface is not large enough. Moreover, when the prototype is placed on the landslide, due to the gravity center, the prototype will also have some flip relative to the slide surface. As the slope increases, the degree of flip could be too large, which would also affect the normal movement, which needs to be considered in the subsequent design.

5.5 Three-segment Prototype Experiments

On the basis of the two-segment prototype, a segment was added to test the effect on the motion of the original structure, as shown in the Fig.51. The experiment found that with reasonable control and control, the three-segment prototype could turn normally, and the speed was reduced a little compared with the original two-segment structure. The results of the experiment are shown in the Tab.5. It can be found that in this experiment, not only the tension of the motor is reduced, but also the values of T1 and

T2 are increased.

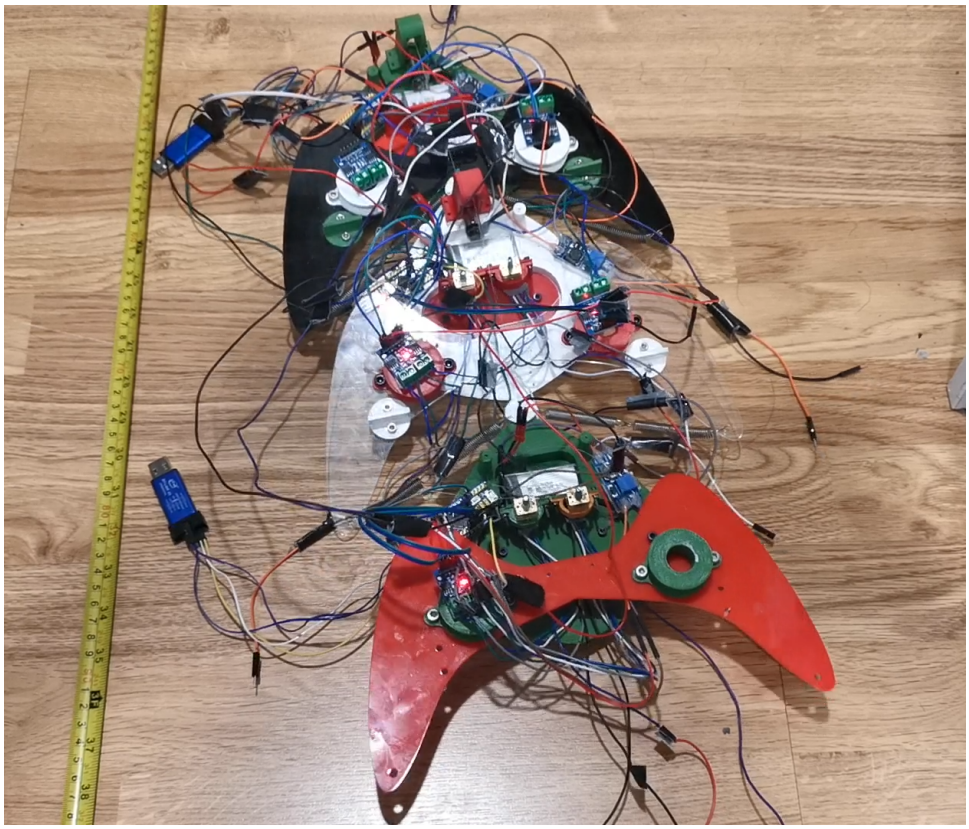

Figure 51: A three-segment prototype

Table 5: The linear motion results of the three-segment prototype

No.	the coefficient of spring	duty cycle of high level (PWM of the motor)	T1(s)	T2(s)	test area	the average speed of prototype (cm/s)
11	small	2/3	1	0.5	floor	1.08
12	small	2/3	1	0.5	paper	1.2

The main reason was that when one segment pulled the other two segments, the tension was limited by friction. In this case, if the tension and the period of motion don't change, the static friction force of the second segment would not be enough to push

the first segment and pull the third, the prototype will go backwards. So the time of pushing the first segment and pulling the third segment could only be staggered to a certain extent. In this experiment, T1 was extended to 1s, which was the motor drive time for the first segment. The motor of the third segment starts after the first segment moves for 0.5s. At this time, the first segment has basically finished its movement and will not exert thrust on the second segment, so the second segment avoids going backwards.

However, if more segments are added, the mass ratio of the kinetic and stationary parts will approach 1, and the friction limit will have less impact on the forward rhythm. Multiple segments will also make the movement of the robotic snake more robust. Thanks to the help of other body segments, each part of the snake can cross more terrains.

5.6 Steering Experiment

In the experiment of steering, it was found that the original design of the structure is not reasonable - Left and right tension directed by the pulleys are difficult to balance in the tensegrity structure. In the actual movement, the original design is difficult to realize the expected change of the structure by accurately finding the right time when one side of the body module is relatively static. This is because the change of the tension in the original design not only changed the balance of left and right sides, in the meantime it will break the tension balance between front and rear segments, making them can't keep the stability (Neither of them can stay static). As a result, the steering movement become invalid - two modules rotate relatively to each other, not rotate by an absolute

angle.

The design was changed later in the experiment, the structure is more simple, as shown in the Fig.52, the red part of the connection part can replace the yellow line connection. It is not difficult to see that in the original connection (yellow line), when the motor in the abdomen of the module tensions the tendon, the pulley guiding the tendon will turn the tension into a push to exert on the second segment forward, making the module unable to maintain the flipped state, and also unable to maintain the friction difference between the modules. The new connection (red line) allows the tension of the tendon to be used for the rotation of the module, but does not affect the relative distance between the modules. After this change, the tension of the left and right motors can more directly affect the tension structure, thus forcing the module to rotate when moving, without affecting the rhythm of the module's linear motion. It has been proved by experiments that this change can improve the rotation of the prototype.

Table 6: The rotation motion results of the three-segment prototype

No.	the coefficient of spring	duty cycle of high level (PWM of the motor)	T1(s)	T2(s)	test area	the average speed of prototype (cm/s)	the average rotation speed of the prototype (°/s)
13	small	2/3	1.2	0.6	floor	1.07	1.71

The result of the steering experiment of the three-section prototype is shown in the Tab.6. The average rotation speed of the prototype was 1.71°/s, and the speed was mainly limited by the size of the rear wing of the module. The size of the rear wing of the module limited the maximum steering angle that the two modules could carry out for each forward step. This makes sense because, in fact, these modules are shaped

like the joints of a snake's spine (as shown in the Fig.53), which can tolerate only small angular changes between the joints, and a greater degree of overall steering is required through many joints.

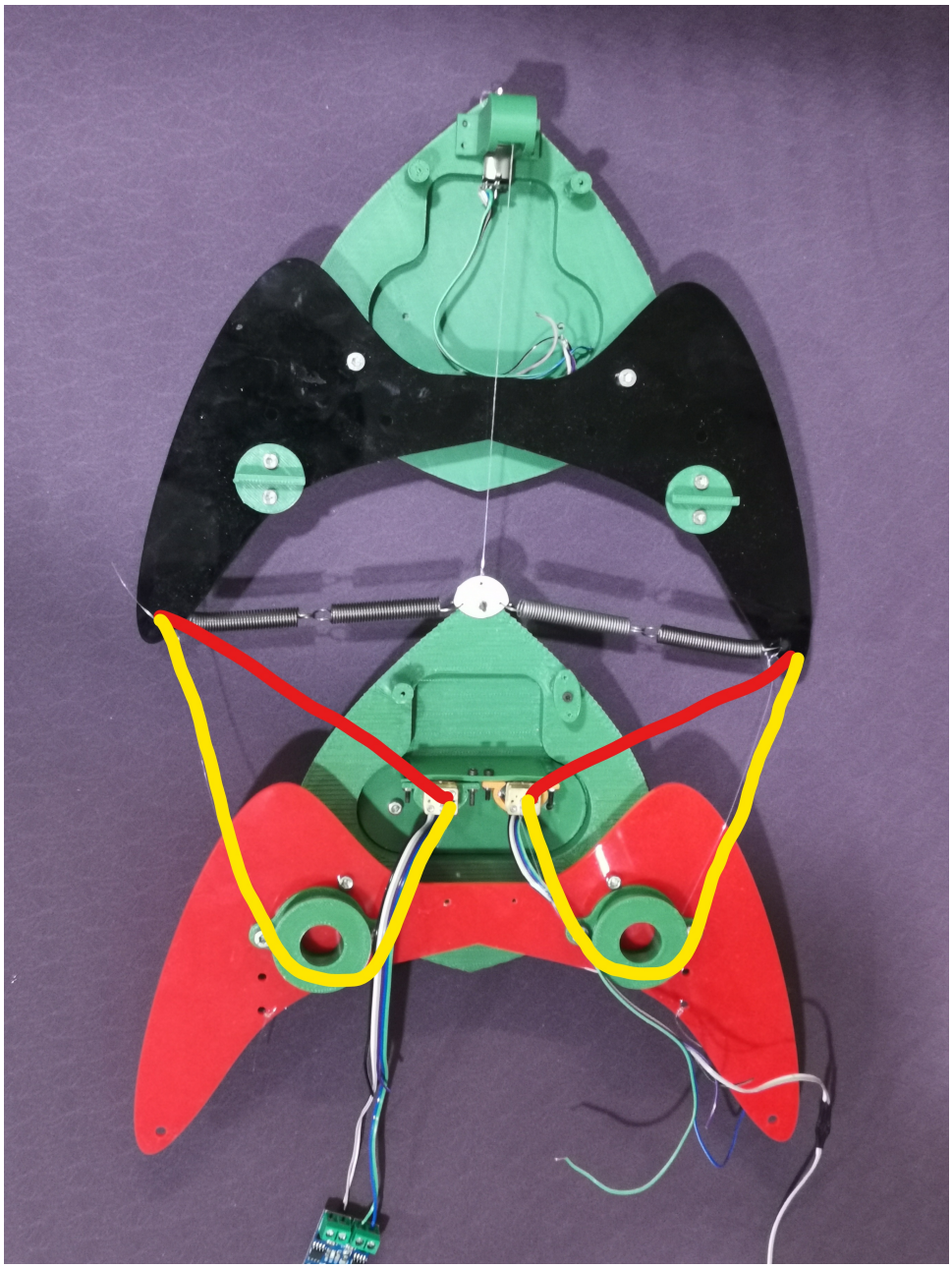

Figure 52: Changes made to tendon connections for better rotation. - The yellow line represents the original tendon connection, and the red line represents the modified tendon connection. It is not difficult to find that after modification, the tendon is directly connected to the motor and the rear wing of the previous module, which has less impact on the relative distance between modules than the original one.

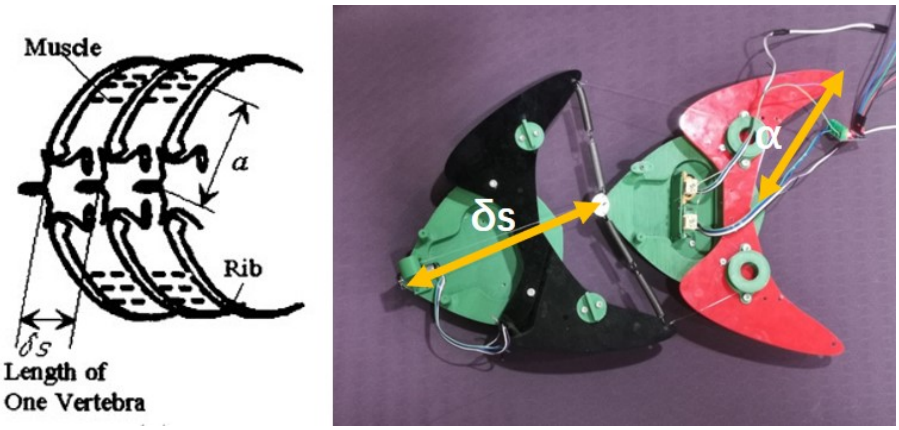

Figure 53: The left part is a schematic diagram of the snake's spine (taken from [31]), and right part is a two-segment prototype for reference

5.7 Transverse Undulating Motion Experiment

The lateral undulating motion experiment was not successful. The three-segment prototype couldn't wiggle its body to force itself forward. Two factors may account for this phenomenon.

One is that the prototype does not have enough segments. Depending on the number of segments, the snake-like robot needs to adopt different motion modes in transverse undulating motion [9]. There are only three sections in the prototype, so it is difficult to realize the lateral undulating motion well. The key to lateral undulation is that snakes can move along the path of S and the resultant force of friction from each landing place is backwards. But the lack of segments causes the landing place to fail to form a complete curve, which causes the whole body to lean to one side, but the whole body cannot move forward.

Second, the bottom design of the prototype module is not well considered. It is difficult to use the friction force in the side direction. The current design of the lower

surface is divided into front and rear lower surfaces, which were designed primarily to accommodate caterpillar movement. However, this design does not make a difference in the left, center and right parts, when the module is forced from the side, the module can not stop steadily (because of the irregular edges). This prevents the module from tilting steadily from the side. But the lateral undulation motion requires lateral friction to move the snake along the path of S. The lower surface should be designed to be spherical, which not only reduces the friction over obstacles [29], but also makes it easier to use the friction in all directions of the body module, making serpentine movement possible. Meanwhile, different materials can still be attached to the lower surface to determine the amount of friction by the tilt of the segment.

6 Conclusions and Future Work

6.1 Conclusions

This project aims to explore a new type of tensegrity robot snake with a structure that better mimics the rectilinear motion of a biological snake. Some video recordings of the experiments can be found at the following link:

https://drive.google.com/drive/folders/1C1m-_3DhP2crb-C3Kvo7XflZRK6m99Zn?usp=sharing

The basic motion of the prototype was carried out on varying terrain with different friction forces. The relationship between the step length, step frequency, the spring and the overall velocity of the prototype were studied by calculation and experiments. Tentative experiments have also been made for special slopes. Here are the main points of the results.

1. The addition of special material to the lower surface of the segment can make the prototype motion more ideal (prevent retrogression).

2. The prototype can complete rectilinear motion on different surfaces. Increasing the tension provided by the motor can increase the step size, which can improve the forward speed of the prototype. The smooth floor is conducive to the increase of step size, but the increase of spring elasticity coefficient cannot significantly improve the speed.

3. The prototype can turn directions, but it is not fast due to the size of the rear wing.

4. Low angle slope is conducive to module flip and improves the overall speed of

the prototype, but over a certain angle the slope will cause the prototype unable to move.

5. During the experiments, the prototype could not perform serpentine movement as expected. Some improvement needs to be continued to make the body able to be twisted to change the side angle of the body to the ground, thus increasing friction. And more segments need to be added.

6.2 Significance of Research

The biggest meaning of this project is to explore the tensegrity structure of a simple snake robot. Compared to other research about tensegrity structures, this project uses flexible connections between modules. In the meantime the structure was reasonably simplified by the use of springs and the ground constraints on the tension structure. This structure realizes rectilinear movement and steering movement of a robotic snake, and also it proves the feasibility of the spring to be used in tension structure systems - With the periodic motion of the spring, the movement of the robotic snake can be more rapid and energy saving.

6.3 Further Work

Future work will focus on mimicking the serpentine movement, which needs to improve the shape of the bottom of each segment. A spherical underside can be tested, allowing the robot snake to effectively utilize the lateral force of each segment of its body.

Miniaturization is also worth trying in the future. The current robot snake is too large, which limits its scope of work. By shrinking the module and increasing the number of

segments in its body, it can perform more tasks and adapt to more terrains.

After increasing the perception of the robotic snake, better travel strategies need to be adopted to improve the basic movement and overall route planning of the robotic snake.

Appendices

1.Matlab: Calculate the speed of the prototype

```
%Set variable value
len = 0.75*pi;
C1 = 1;
K = 1;
M = 1;
T0_10 = 0.1;
T0_11 = 1;
T0_12 = 10;

%Calculate speed and distance according to time
pt=0:0.1:len;
distance = -(C1/(2*K))*cos(sqrt(2*K/M)*pt)+C1/(2*K);
averagespeed0 = (distance)./(T0_10+pt);
averagespeed1 = (distance)./(T0_11+pt);
averagespeed2 = (distance)./(T0_12+pt);
Ft = (C1 - 2*K*distance);
ps = 0:0.05:1;
Fs = C1 - 2*K*ps;

%Draw diagrams
subplot(4,1,1);
```

```
plot(ps,Fs,'r');
xlabel("s1(m)");
ylabel("Fpull(N)");
title('The tension applied to the module varies with distance during the
legend('Tension');

subplot(4,1,2);
plot(pt,Ft,'r');
xlabel("t1(s)");
ylabel("Fpull(N)");
title('The tension applied to the module varies with time during the pull
legend('Tension');

subplot(4,1,3);
plot(pt,distance,'r');
xlabel("t1(s)");
ylabel("s1(m)");
title('Distance traveled by the module varies with time during the pull s
legend('Distance');

subplot(4,1,4);
plot(pt,averagespeed0,'g',pt,averagespeed1,'b',pt,averagespeed2,'y');
xlabel("T1(s)");
```

```
ylabel("Average speed(m/s)");
title({'The average velocity of prototype during the pull stage varies wi
legend('T0_1=0.1s','T0_2=1s','T0_3=10s');
```

Part program of three-segment prototype

Motion plan list

```
//Each line corresponds to the duration(ms) and motor PWM setting
int state_machine[100] = {
10000,150,100,0,600,-100,0,
600,600,-100,0,-150,100,0,
600,600,-100,0,600,-100,0,
600,-150,100,0,600,-100,0,
600,600,-100,0,-150,100,0,
600,600,-100,0,600,-100,0,
600,-150,100,0,600,-100,0,
};
```

2.Motor state initialization:

```
//Record the initial state and setting value of the motor
MotorState MotorInitialTable[9] =
{KEEPTENSION,KEEPTENSION,KEEPTENSION,
RELAX,RELAX,RELAX,
```

```
RELAX,RELAX,RELAX};
int MotorInitialTable1[9] = {100,0,0,
                             0,0,0,
                             0,0,0};
int MotorInitialTable2[9] = {0,0,0,
                             0,0,0,
                             0,0,0};

//Load corresponding value
void MotorInitialSetting()
{
    DriveMotorState.MState = MotorInitialTable[BoardNumber];
    DriveMotorState.tension_value = MotorInitialTable1[BoardNumber];
    DriveMotorState.position_value = MotorInitialTable2[BoardNumber];

    LeftMotorState.MState = MotorInitialTable[BoardNumber+1];
    LeftMotorState.tension_value = MotorInitialTable1[BoardNumber+1];
    LeftMotorState.position_value = MotorInitialTable2[BoardNumber+1];

    RightMotorState.MState = MotorInitialTable[BoardNumber+2];
    RightMotorState.tension_value = MotorInitialTable1[BoardNumber+2];
    RightMotorState.position_value = MotorInitialTable2[BoardNumber+2];
}
```

Execute corresponding motion:

```
//Load parameters
void ExcutePlan()
{
    ExcuteMotorState(&DriveMotorState,&DriveMotor);
    ExcuteMotorState(&LeftMotorState,&LeftMotor);
    ExcuteMotorState(&RightMotorState,&RightMotor);
}

//Setup parameters
void ExcuteMotorState(MotorStateTypeDef *MotorState,MotorTypeDef *Motor)
{
    switch((*MotorState).MState)
    {
        case RELAX:
            (*Motor).State = MOTOR_PWM;
          (*Motor).PWMExpected = 0;
            break;
        case KEEPTENSION:
            (*Motor).State = MOTOR_PWM;
          (*Motor).PWMExpected = (*MotorState).tension_value;
            break;
```

```
        case KEEPPOSITION:
            (*Motor).State = PIDPOSITION;
          (*Motor).PositionExpected = (*MotorState).position_value;
            break;
        default:
            break;
    }
}

//Set the output corresponding PWM wave
void basic_control(int motor_number, int value)
{
        switch(motor_number)
        {
                case 1:
                {
                        if(speed>0)
                        {
                                TIM_SetCompare1(TIM2,value);
                                TIM_SetCompare2(TIM2,0);
                        }
                        else
                        {
```

```
                TIM_SetCompare2(TIM2,-value);
                TIM_SetCompare1(TIM2,0);
            }
        }
        break;

    case 2:
        if(speed>0)
        {
            TIM_SetCompare1(TIM3,value);
            TIM_SetCompare2(TIM3,0);
        }
        else
        {
            TIM_SetCompare2(TIM3,-value);
            TIM_SetCompare1(TIM3,0);
        }
        break;

    case 3:
        if(speed>0)
        {
            TIM_SetCompare3(TIM3,value);
```

```
                    TIM_SetCompare4(TIM3,0);
                }
                else
                {
                    TIM_SetCompare4(TIM3,-value);
                    TIM_SetCompare3(TIM3,0);
                }
                break;

            default:
                break;
        }
}
```

Send and receive broadcasts:

```
//Send broadcasts

void ExcuteMachineState(void)
{
//The snakehead module sends the broadcast,
//and the body module executes the broadcast
            #ifdef first_broad
```

```
int i = 0;
    int j = 0;
    //Execute continuously according to the form plan
    switch(ThePlan)
    {
            case ASPLAN:
                    if(state_machine[current_plan_state*
                    (motor_number+1)]==0)
                    //Over schedule forms
                   {
                           current_plan_state = 1;
                   }
                   else//In the plan
                   {
                   if(getclock()-state_start_time>=state_machine
                   [current_plan_state*(motor_number+1)]*10)
                           {
                                   state_start_time = getclock();
                                   current_plan_state ++;
                           }
                           Send_Message(USART1,'#');
                           for( ;i<motor_number;i++)
                           {
```

```
                    //Send broadcasts
 Send_Message(USART1,state_machine
 [current_plan_state*(motor_number+1)+1+i]
 /10+change_value/10);
                    }
                    Send_Message(USART1,'!');
                    DriveMotorState.MState = KEEPTENSION;
DriveMotorState.tension_value =
state_machine[current_plan_state*
(motor_number+1)+1];
          }
          break;

//PC side instruction is required to
//switch motion state for debugging
case ASSTATICPLAN:
          j = message[1] - '0';
          if(j>90)//Over schedule forms
          {
                    j = 0;
          }
          else//In the plan
          {
```

```
                    Send_Message(USART1,'#');
                    for( ;i<motor_number;i++)
                    {
                //Send broadcasts
            Send_Message(USART1,static_state_machine
                [j*(motor_number+1)+1+i]/10+change_value/10);
                    }
                    Send_Message(USART1,'!');
                    DriveMotorState.MState = KEEPTENSION;
        DriveMotorState.tension_value =
        static_state_machine[j*(motor_number+1)+1];
                }
                break;

        default:
                break;
}

//The body segment only needs to set
//parameters according to the broadcast content
                #else
          DriveMotorState.MState = KEEPTENSION;
      DriveMotorState.tension_value = straight_motor_value;
```

```
                LeftMotorState.MState = KEEPTENSION;
                LeftMotorState.tension_value = left_motor_value;

                RightMotorState.MState = KEEPTENSION;
                RightMotorState.tension_value = right_motor_value;
    #endif
}


//receive broadcasts
void USART1_IRQHandler(void)
        {
        u8 Res;
        if(USART_GetITStatus(USART1, USART_IT_RXNE) != RESET)
                {
                Res =USART_ReceiveData(USART1);

                //The body segments needs to read the broadcast
                #ifndef first_broad
                  //message[1] = Res;
                if(Res == '!')
                {
```

```
                plan_start = false;
                message_number = 0;
            }
            if(plan_start)
            {
            //Record the parameters in the broadcast content
            if(message_number == 3*broad_number-5+1)
            left_motor_value = 10*judgedirection(Res);

            if(message_number == 3*broad_number-5+2)
            right_motor_value = -10*judgedirection(Res);

            if(message_number == 3*broad_number-5+3)
            straight_motor_value = 10*judgedirection(Res);
            message_number++;
            }
            #endif
    }
    USART_ClearITPendingBit(USART1,USART_IT_RXNE);
}
```

3.Supplementary derivation of the equation 6 and 9

In the simplified prototype mathematical model, the force is in the same horizontal plane without considering the variation of the pitch angle of the prototype. It can be

known that:

$$F_{pull} = F_1 - f - 2k \triangle l \cos\theta$$

$$= C_1 - 2k \triangle s_1$$

$$\begin{aligned}
\triangle s_1 &= \int_0^{T_1} v_{prototype} \mathrm{d}t \\
&= \int_0^{T_1} \mathrm{d}t_1 \int_0^{T_1} a_{prototype} \mathrm{d}t_1 \\
&= \int_0^{T_1} \mathrm{d}t_1 \int_0^{T_1} \frac{F_{pull}}{m} \mathrm{d}t_1 \\
&= \int_0^{T_1} \mathrm{d}t_1 \int_0^{T_1} \frac{C_1 - 2k \triangle s_1}{m} \mathrm{d}t_1
\end{aligned}$$

F_{pull} is the resultant force on the mobile module of the prototype in the pull stage, C_1 represents a fixed constant, depending on the tension (F_1) and the ground friction of the mobile module (f), k is the elastic coefficient of spring, $\triangle l$ is the change in length of the spring compared to the original length, θ is the angle between the spring and the forward direction of the module (acute Angle), $\triangle s_1$ is the moving distance of the mobile module in the pull stage, T_1 is the time of the pull phase, $v_{prototype}$ is the speed of the mobile module, $a_{prototype}$ is the acceleration of the mobile module, m represents the quality of the mobile module, t_1 represents the time from the start of the pull phase to the present.

Since $\triangle s_1$ can be obtained by double integration of an expression with $\triangle s_1$, we can

assume that $\triangle s_1$ is of the following form (A, B, C, D, E, t_0 are unknowns, $t_0 \in [0, 2\pi)$):

$$\Delta S_1 = A\cos(Bt_1 + t_0) + Ct^2 + Dt_1 + E$$

$$\Delta S_1{}' = -AB\sin(Bt_1 + t_0) + 2Ct_1 + D$$

$$\Delta S_1{}'' = -AB^2\cos(Bt_1 + t_0) + 2C$$

Based on the relationship between acceleration and distance and the boundary conditions (initial distance ($\triangle s_1$) and initial velocity ($v_{prototype}$) are 0), the following relationship can be obtained:

$$\begin{cases} \Delta s_1{}'' & = a_{prototype} = \frac{F_{pull}}{m} \\ \Delta s_{1|t_1=0} = 0 & \\ \Delta s_1{}'_{|t_1=0} & = v_{prototype|t_1=0} = 0 \end{cases}$$

$$\Rightarrow \begin{cases} -AB^2\cos(Bt_1 + t_0) + 2C & = \frac{C_1}{m} - \frac{2k}{m}(A\cos(Bt_1 + t_0) + Ct_1^2 + Dt_1 + E) \\ A\cos(t_0) + E & = 0 \\ -AB\sin(t_0) + D & = 0 \end{cases}$$

$$\Rightarrow \begin{cases} (-AB^2 + \frac{2k}{m}A)\cos(Bt_1 + t_0) + \frac{2k}{m}(Ct_1^2 + Dt_1) + 2C - \frac{C_1}{m} + \frac{2k}{m}E & = 0 \\ A\cos(t_0) + E & = 0 \\ -AB\sin(t_0) + D & = 0 \end{cases}$$

$$\Rightarrow \begin{cases} (-B^2+\frac{2k}{m}) & =0 \\ \frac{2k}{m}C & =0 \\ \frac{2k}{m}D & =0 \\ 2C-\frac{C_1}{m}+\frac{2k}{m}E & =0 \\ -AB\sin(t_0)+D & =0 \\ A\cos(t_0)+E & =0 \end{cases} \Rightarrow \begin{cases} B & =\sqrt{\frac{2k}{m}} \\ C & =0 \\ D & =0 \\ -\frac{C_1}{m}+\frac{2k}{m}E & =0 \\ \sin(t_0) & =0 \\ A+E & =0 \end{cases}$$

$$\Rightarrow \begin{cases} A & =-\frac{C_1}{2k} \\ B & =\sqrt{\frac{2k}{m}} \\ C & =0 \\ D & =0 \\ E & =\frac{C_1}{2k} \\ t_0 & =0 \end{cases} or \begin{cases} A & =\frac{C_1}{2k} \\ B & =\sqrt{\frac{2k}{m}} \\ C & =0 \\ D & =0 \\ E & =\frac{C_1}{2k} \\ t_0 & =\pi \end{cases}$$

The result above shows that:

$\triangle s_1 = -\frac{C_1}{2k}\cos(\sqrt{\frac{2k}{m}}t_1)+\frac{C_1}{2k}$ or $\triangle s_1 = \frac{C_1}{2k}\cos(\sqrt{\frac{2k}{m}}t_1+\pi)+\frac{C_1}{2k}$

Since the mobile module in the pull stage will end its motion before $\triangle s_1$ reaches the maximum value and switch to the push stage (avoiding invalid move, namely, moving back), it can be further known that:

$$\triangle s_1 = -\frac{C_1}{2k}\cos(\sqrt{\frac{2k}{m}}t_1)+\frac{C_1}{2k}(\sqrt{\frac{2k}{m}}t_1 \in [0,\pi])$$

$$\triangle s_1 = \frac{C_1}{2k}\cos(\sqrt{\frac{2k}{m}}t_1+\pi)+\frac{C_1}{2k}(\sqrt{\frac{2k}{m}}t_1 \in [0,\pi])$$

These two equations are essentially the same, and the rest of the statement is

written in terms of the first equation.

In the push stage,

$$F_{push} = C_2 - 2k \triangle s_2$$

$$C_2 = 2kS_{1max} - f$$

F_{push} is the resultant force on the mobile module of the prototype in the push stage, $\triangle s_2$ is the moving distance of the mobile module in the push stage. S_{1max} is the distance traveled in the pull stage, so $C2$ and $C1$ both are essentially a certain constant, the derivation of $\triangle s_2$ and $\triangle s_1$ is exactly the same. By substituting C1 with C2, we can get the following equation:

$$\triangle s_2 = -\frac{C_2}{2k}\cos(\sqrt{\frac{2k}{m}}t_2) + \frac{C_2}{2k}(\sqrt{\frac{2k}{m}}t_2 \in [0, \pi])$$

References

[1] Rectilinear Locomotion in a Snake (Boa Occidentalis). *Journal of Experimental Biology*, 26(4):368–379, 1950.

[2] J. B. Aldrich and R. E. Skelton. Backlash-free motion control of robotic manipulators driven by tensegrity motor networks. In *Proceedings of the IEEE Conference on Decision and Control*, pages 2300–2306, 2006.

[3] J. B. Aldrich, R. E. Skelton, and K. Kreutz-Delgado. Control Synthesis for a Class of Light and Agile Robotic Tensegrity Structures. In *Proceedings of the American Control Conference*, volume 6, pages 5245–5251, 2003.

[4] Z. Y. Bayraktaroglu. Snake-like locomotion: Experimentations with a biologically inspired wheel-less snake robot. *Mechanism and Machine Theory*, 2009.

[5] C. Branyan, C. Fleming, J. Remaley, A. Kothari, K. Tumer, R. L. Hatton, and Y. Menguc. Soft snake robots: Mechanical design and geometric gait implementation. In *2017 IEEE International Conference on Robotics and Biomimetics, ROBIO 2017*, volume 2018-Janua, pages 282–289, 2018.

[6] F. Carreño and M. A. Post. Design of a novel wheeled tensegrity robot: a comparison of tensegrity concepts and a prototype for travelling air ducts. *Robotics and Biomimetics*, 5(1), 2018.

[7] P. Chavan, M. Murugan, E. V. Unnikkannan, A. Singh, and P. Phadatare. Modular snake robot with mapping and navigation: Urban search and rescue (USAR) robot. In *Proceedings - 1st International Conference on Computing, Commu-*

nication, Control and Automation, ICCUBEA 2015, pages 537–541. Institute of Electrical and Electronics Engineers Inc., 7 2015.

[8] P. Y. Chen, J. McKittrick, and M. A. Meyers. Biological materials: Functional adaptations and bioinspired designs, 2012.

[9] F. L. Chernousko. Modelling of snake-like locomotion. In *Applied Mathematics and Computation*, volume 164, pages 415–434, 5 2005.

[10] R. Connelly and A. Back. Mathematics and Tensegrity. *American Scientist*, 1998.

[11] Coral-snake.com. Snake locomotion.

`http://www.coral-snake.com/body-structure/coral-snake-locomotion-movement.html`.

[12] K. Dowling. Limbless locomotion: Learning to crawl with a snake robot. *Ph.D.dissertation*, 1997.

[13] W. Du, S. Ma, B. Li, M. Wang, and S. Hirai. Force Analytic Method for Rolling Gaits of Tensegrity Robots. *IEEE/ASME Transactions on Mechatronics*, 21(5):2249–2259, 10 2016.

[14] B. Duperron. Illustration about sidewinding movement.

`https://www.guwsmedical.info/photo-animals/skeleton-muscle-and-movement.html`.

[15] E. Fest, K. Shea, and I. F. Smith. Active tensegrity structure. *Journal of Structural Engineering*, 130(10):1454–1465, 10 2004.

[16] J. Gao, X. Gao, W. Zhu, J. Zhu, and B. Wei. Design and research of a new structure rescue snake robot with all body drive system. In *Proceedings of 2008 IEEE International Conference on Mechatronics and Automation, ICMA 2008*, pages 119–124, 2008.

[17] Z. V. Guo and L. Mahadevan. Limbless undulatory propulsion on land. *Proceedings of the National Academy of Sciences of the United States of America*, 105(9), 2008.

[18] P. M. He Q. An Adaptable Robotic Snake Using a Compliant Actuated Tensegrity Structure for Locomotion. *Towards Autonomous Robotic Systems. TAROS 2020. Lecture Notes in Computer Science*, 12228:70–74, 2020.

[19] S. Hirose and E. F. Fukushima. Snakes and strings: New robotic components for rescue operations. In *International Journal of Robotics Research*, volume 23, pages 341–349, 4 2004.

[20] S. Hirose and M. Mori. Biologically inspired snake-like robots. In *Proceedings - 2004 IEEE International Conference on Robotics and Biomimetics, IEEE ROBIO 2004*, pages 1–7, 2004.

[21] D. E. Ingber. Tensegrity I. Cell structure and hierarchical systems biology, 4 2003.

[22] V. R. J. Sitár and . TnUAD. *Industrial Electronics and Applications, 2008, ICIEA 2008, 3rd IEEE Conference on : date, 3-5 June 2008.* IEEE Xplore, 2008.

[23] V. G. Jáuregui. *Tensegrity Structures and their Application to Architecture*. 2004.

[24] A. Kakogawa, S. Jeon, and S. Ma. Stiffness Design of a Resonance-Based Planar Snake Robot with Parallel Elastic Actuators. *IEEE Robotics and Automation Letters*, 3(2):1284–1291, 4 2018.

[25] T. Kamegawa, T. Harada, and A. Gofuku. Realization of cylinder climbing locomotion with helical form by a snake robot with passive wheels. In *Proceedings - IEEE International Conference on Robotics and Automation*, pages 3067–3072, 2009.

[26] T. Khunnithiwarawat and T. Maneewarn. A study of Active-Wheel snake robot locomotion gaits. In *2011 IEEE International Conference on Robotics and Biomimetics, ROBIO 2011*, pages 2805–2809, 2011.

[27] konvat. Did you know these reptiles move around in four different ways?

`https://www.nairaland.com/5131233/did-know-these-reptiles-move`.

[28] B. Lab. Concertina motion of snake.

`https://images.app.goo.gl/VVAwj5wjYHDKyYkk6`.

[29] P. Liljebäck, K. Y. Pettersen, Stavdahl, and J. T. Gravdahl. Snake robot locomotion in environments with obstacles. *IEEE/ASME Transactions on Mechatronics*, 17(6):1158–1169, 2012.

[30] C. Lin, D. Li, and Y. Zhao. Tensegrity robot dynamic simulation and kinetic strategy programming. In *CGNCC 2016 - 2016 IEEE Chinese Guidance, Navigation and Control Conference*, pages 2394–2398. Institute of Electrical and Electronics Engineers Inc., 1 2017.

[31] S. Ma. Analysis of snake movement forms for realization of snake-like robots. *Proceedings - IEEE International Conference on Robotics and Automation*, 4:3007–3013, 1999.

[32] H. Marvi, J. Bridges, and D. L. Hu. Snakes mimic earthworms: Propulsion using rectilinear travelling waves. *Journal of the Royal Society Interface*, 10(84), 2013.

[33] H. Marvi, J. P. Cook, J. L. Streator, and D. L. Hu. Snakes move their scales to increase friction. *Biotribology*, 5:52–60, 3 2016.

[34] M. A. Meyers, J. McKittrick, and P. Y. Chen. Structural biological materials: Critical mechanics-materials connections, 2 2013.

[35] J. M. Mirats Tur, S. Hernàndez Juan, and A. Graells Rovira. Dynamic equations of motion for a 3-bar tensegrity based mobile robot. Technical report, 2007.

[36] M. Mori and S. Hirose. Development of active cord mechanism ACM-R3 with agile 3D mobility. In *IEEE International Conference on Intelligent Robots and Systems*, volume 3, pages 1552–1557, 2001.

[37] S. J. Newman and B. C. Jayne. Crawling without wiggling: Muscular mechanisms and kinematics of rectilinear locomotion in boa constrictors. *Journal of Experimental Biology*, 221(4), 2018.

[38] S. J. Oh, H. J. Kwon, J. Lee, and H. Choi. Mathematical modeling for omni-tread type snake robot. In *ICCAS 2007 - International Conference on Control, Automation and Systems*, 2007.

[39] B. Oraw. Design report 1 modular snake robot.

https://www.researchgate.net/figure/Lateral-Undulation-Motion_fig6_255672289.

[40] K. L. Paap, T. Christaller, and F. Kirchner. A robot snake to inspect broken buildings. *IEEE International Conference on Intelligent Robots and Systems*, 3:2079–2082, 2000.

[41] K. Y. Pettersen. Snake robots, 2017.

[42] A. Rezaei, Y. Shekofteh, M. Kamrani, A. Fallah, and F. Barazandeh. Design and control of a snake robot according to snake anatomy. In *Proceedings of the International Conference on Computer and Communication Engineering 2008, ICCCE08: Global Links for Human Development*, pages 191–194, 2008.

[43] Sajjad Manzoor and Youngjin Choi. *Modular Design of Snake Robot for Various Motions Implementation*. 2016.

[44] Y. Shan and Y. Koren. Design and Motion Planning of a Mechanical Snake. *IEEE Transactions on Systems, Man and Cybernetics*, 23(4):1091–1100, 1993.

[45] K. Snelson. The art of tensegrity. *International Journal of Space Structures*, 2012.

[46] T. D. Ta, T. Umedachi, and Y. Kawahara. Design of Frictional 2D-Anisotropy Surface for Wriggle Locomotion of Printable Soft-Bodied Robots. In *Proceedings - IEEE International Conference on Robotics and Automation*, pages 6779–6785. Institute of Electrical and Electronics Engineers Inc., 9 2018.

[47] M. Tanaka and F. Matsuno. Experimental study of redundant snake robot based on kinematic model. In *Proceedings - IEEE International Conference on Robotics and Automation*, pages 2990–2995, 2007.

[48] L. Tang, L. M. Zhu, X. Zhu, and G. Gu. A Serpentine Curve Based Motion Planning Method for Cable-Driven Snake Robots. In *Proceedings of the 2018 25th International Conference on Mechatronics and Machine Vision in Practice, M2VIP 2018*, 2019.

[49] B. R. Tietz, R. W. Carnahan, R. J. Bachmann, R. D. Quinn, and V. Sunspiral. Tetraspine: Robust terrain handling on a tensegrity robot using central pattern generators. In *2013 IEEE/ASME International Conference on Advanced Intelligent Mechatronics: Mechatronics for Human Wellbeing, AIM 2013*, 2013.

[50] A. A. Transeth, P. Liljebäck, and K. Y. Pettersen. Snake robot obstacle aided locomotion: An experimental validation of a non-smooth modeling approach. In *IEEE International Conference on Intelligent Robots and Systems*, pages 2582–2589, 2007.

[51] W. Wang, A. Ji, P. Manoonpong, H. Shen, J. Hu, Z. Dai, and Z. Yu. Lateral undulation of the flexible spine of sprawling posture vertebrates, 2018.

[52] X. Ye, Y. Niu, H. Wang, and T. Meng. Locomotion control for a modular snake robot over rough terrain. In *2010 2nd Conference on Environmental Science and Information Application Technology, ESIAT 2010*, volume 2, 2010.